ELSEVIER

Inorganica Chimica Acta 279 (1998) 7–23

Inorganica Chimica Acta

Protonation of Fischer-type alkylidyne carbonyltungsten complexes. Structural comparison of alkylidyne and alkylidene metal complexes, including a neutron diffraction study of $[W(CHCH_3)Cl_2(CO)(PMe_3)_2]$

Cecilia M. Bastos [a], Ken S. Lee [a,1], Michael A. Kjelsberg [d], Andreas Mayr [a,b,*], Donna Van Engen [d], Stephen A. Koch [a], John D. Franolic [a], Wim T. Klooster [c], Thomas F. Koetzle [c]

[a] *Department of Chemistry, State University of New York at Stony Brook, Stony Brook, NY 11794-3400, USA*
[b] *Department of Chemistry, The University of Hong Kong, Pokfulam Road, Hong Kong, China*
[c] *Department of Chemistry, Brookhaven National Laboratory, PO Box 5000, Upton, NY 11973-5000, USA*
[d] *Department of Chemistry, Princeton University, Princeton, NJ 08544, USA*

Received 26 June 1997; accepted 30 July 1997

Abstract

Protonation of alkylidyne tungsten complexes of the types $[W(CR)Cl(CO)(PMe_3)_3]$ or $[W(CR)Cl(CO)(py)(PMe_3)_2]$ with HCl affords the η^2-alkylidene tungsten complexes $[W(CHR)Cl_2(CO)(PMe_3)_2]$ (**7**) (R = Me, Et, Ph, *p*-Tol). Protonation of the complexes $[W(CR)X(CO)(CNR')(PMe_3)_2]$ with $HOSO_2CF_3$ or HBF_4 gives the alkylidene complexes $[W(CHR)X(CO)(CNR')(PMe_3)_2][Y]$ (**8**) (R = Me, R' = CMe_3, X = Cl, Y = CF_3SO_3, R = Ph, X = Cl; R' = CMe_3, Y = CF_3SO_3, BF_4; R' = C_6H_{11}, Y = BF_4; R' = $C_6H_3Me_2$-2,6, Y = CF_3SO_3, R = Ph, R' = CMe_3, X = I, Y = CF_3SO_3, BF_4). The C–H bonds of the alkylidene ligands are easily deprotonated with bases such as pyrrolidinocyclopentene or triethylamine. The solid state structures of $[W(CPh)Cl(CO)(CNCMe_3)(PMe_3)_2]$ (**5b**), $[W(CHMe)Cl_2(CO)(PMe_3)_2]$ (**7a**), $[W(CHPh)Cl_2(CO)(PMe_3)_2]$ (**7c**), and $[W(CHPh)Cl(CO)(CNCMe_3)(PMe_3)_2][BF_4]$ (**8c**) were determined by X-ray crystallography. The structure of **7a** was also determined by neutron diffraction. Based on the neutron diffraction data of **7a**, and closely matching results from the X-ray diffraction studies, it is found that the η^2-coordination mode of the alkylidene ligands gives rise to almost equal W–C(R) and W–H bond distances, 1.857(4) and 1.922(6) Å, respectively, in the case of **7a**. The length of the alkylidene C–H bond in **7a** is 1.185(7) Å. The structural comparison of **5b** and **8c** reveals that the protonation of the alkylidyne ligand causes the W–CPh bond to lengthen by less than 0.1 Å and the W–C–Ph angle to bend by about 15°. The major induced structural change, however, may be described as a lateral shift of the CPh group by about 0.6 Å away from the coordination axis defined by the extension of the Cl–W vector.

Keywords: Crystal structures; Neutron diffraction; Alkylidene complexes; Tungsten complexes

1. Introduction

Protonation is an effective means of activating Fischer-type alkylidyne complexes towards bond-forming steps [1]. For example, reaction of the complexes $[W(CR)(\eta^5\text{-}C_5H_5)(CO)L]$ (R = alkyl, aryl; L = CO, phosphine, phosphite) with HCl provides η^2-acyl complexes of the type $[W(\eta^5\text{-}C_5H_5)(\eta^2\text{-}OCCH_2R)Cl_2L]$ [2], protonation with HBF_4 affords the dinuclear μ-alkyne complexes $[(W(\eta^5\text{-}C_5H_5)(CO)_2)_2(\mu\text{-}H)(\mu\text{-}RCCR)][BF_4]$ [3], and treatment with HBF_4 in the presence of PhCCPh gives the allylidene complex $[W(CPhCPhCHR)(\eta^5\text{-}C_5H_5)(CO)][BF_4]$ (R = C_6H_4Me-4) and further products [4]. Protonation of alkylidyne isocyanide metal complexes causes the formation of aminoalkyne metal complexes [1i,5], and treatment of alkylidyne carbaborane metal complexes with acids leads to a variety of transformations involving both the alkylidyne and the carbaborane groups [6]. Because of their high reactivity, only few simple protonation products of alkylidyne metal complexes, either alkylidene or alkylidyne hydrido metal complexes, have been isolated [3,7,8]. Evidently, the outcome of protonation reactions depends very strongly on the particular electronic and steric properties of the alkylidyne

* Corresponding author: Tel.: +1-516-632 7951; fax: +1-516-632 7960.
[1] Current address: Department of Chemistry, Jackson State University, Jackson, MS 39217, USA.

0020-1693/98/$19.00
PII S0020-1693(98)00004-8

complexes, the nature of the acid, and the reaction conditions. However, in most cases, if not all, alkylidene metal complexes are involved as the initial protonation products and as key intermediates.

In this paper, we give a full account of the formation of neutral and cationic η^2-alkylidene complexes upon protonation of some Fischer-type alkylidyne tungsten complexes [9,10]. The molecular structures of three representative η^2-alkylidene tungsten complexes as well as the structure of one of the alkylidyne complex precursors have been determined by X-ray crystallography. The structure of one alkylidene tungsten complex has also been studied by neutron diffraction. The comparison of these structures provides insight into the structural changes induced by the protonation of alkylidyne metal complexes and the bonding of the generated η^2-alkylidene ligands.

2. Results

2.1. Synthesis of the alkylidyne and alkylidene complexes

The reactions involved in the synthesis of the alkylidyne complexes **1–5** are well established and are summarized in Scheme 1. Starting from tungsten hexacarbonyl, the bis-pyridine-substituted complexes **1a–e** are obtained by addition of organyllithium reagents, followed by oxalyl chloride and pyridine [11,12]. Substitution of the two pyridine ligands in **1a–e** affords the bis-trimethylphosphine complexes **2a–e**. The tris-trimethylphosphine derivatives **3a–d** are obtained from **2a–d** by irradiation in the presence of trimethylphospine or by treatment with neat PMe_3 [13]. Complex **3a** has previously been obtained by Mayer and coworkers by treatment of $[W(CMe)Cl(PMe_3)_4]$ with carbon monoxide [14]. Substitution of the central trimethylphosphine ligand in complexes **3a** and **3c** by isocyanides gives the complexes **5a–d**. An alternative route to complexes **5** proceeds via the pyridine-substituted compounds **4**, which are obtained by irradiation of the corresponding complexes **1** in the presence of two equivalents of PMe_3 and excess pyridine. Exchange of chloride by iodide in **5b** affords the iodo derivative **6** (Eq. (1)) [15].

The identity of the alkylidyne complexes was established by spectroscopic methods. The *cis*-dicarbonyl compounds **1** and **2** exhibit two IR absorptions of similar intensity in the metal carbonyl region, while only a single absorption is observed for complexes **3–6**. The presence of two mutually *trans* trimethylphosphine ligands in complexes **3–6** is indicated by the appearance of the ^1H NMR resonances of the PMe_3 ligands as virtual triplets. The central PMe_3 ligand in complexes **3** gives rise to an additional doublet. The alkylidyne carbon atoms resonate in the range of δ 250–300.

When a light stream of HCl gas is blown over stirred solutions of complexes **3** and **4** in CH_2Cl_2, the color changes from yellow to dark brown, and the alkylidene complexes **7a–d** form in high yield (Eq. (2)). After removal of the

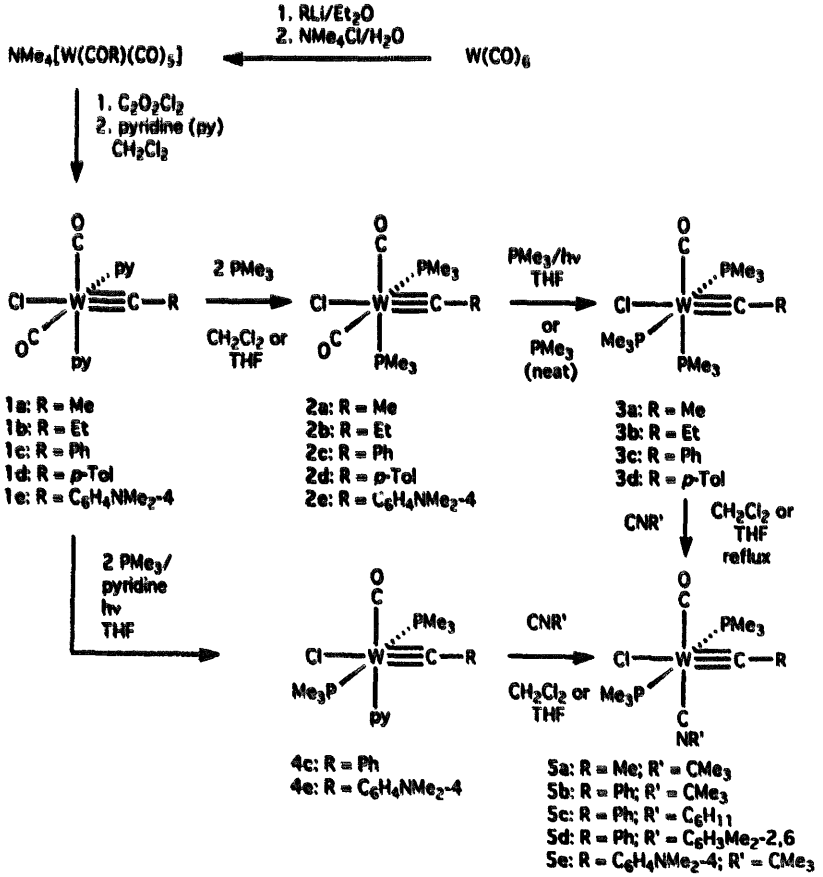

Scheme 1.

solvent, the brown products are extracted with THF or ether and purified either by recrystallization or by chromatography. As demonstrated for **7c**, the alkylidene complexes can also be obtained in high yield, if conc. HCl is used instead of HCl gas. Complexes **7** are moderately air-sensitive in solution, but crystalline samples can be exposed to air for extended periods of time without significant decomposition. The neopentylidene complex $[W(CHCMe_3)Cl_2(CO)(PMe_3)_2]$ (**7e**) has previously been prepared by Schrock and coworkers by treatment of $[W(CHCMe_3)Cl_3H(PMe_3)_2]$ or $[W(CCMe_3)Cl_2H(PMe_3)_2]$ with carbon monoxide [16]. Addition of $HOSO_2CF_3$ or HBF_4 to ether solutions of the isocyanide-substituted alkylidyne complexes **5a–d** and **6** causes the precipitation of the salts **8** which are isolated in nearly quantitative yield after decantation of the supernatant, washing of the residue with hexane, and drying under vacuum (Eq. (3)). The alkylidene complexes **8** are very sensitive towards moisture.

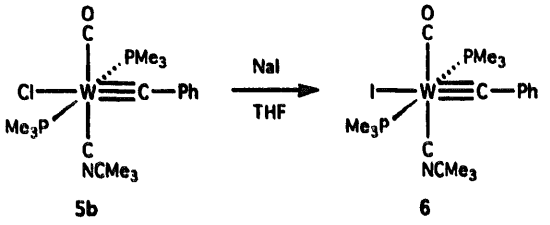

5b **6** (1)

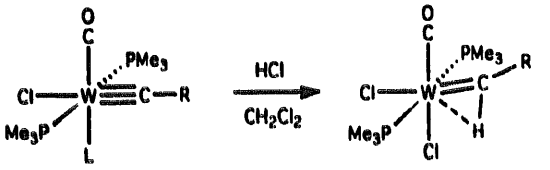

3a-d
4c

7a: R = Me
7b: R = Et
7c: R = Ph
7d: R = *p*-Tol

(2)

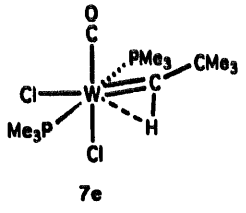

7e

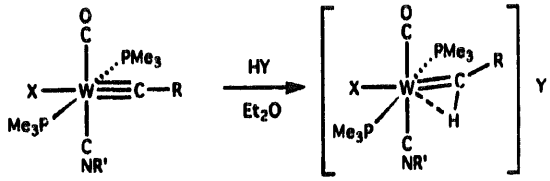

5a-d
6

8a: R = Me; R' = CMe_3; X = Cl; Y = CF_3SO_3
8b: R = Ph; R' = CMe_3; X = Cl; Y = CF_3SO_3
8c: R = Ph; R' = CMe_3; X = Cl; Y = BF_4
8d: R = Ph; R' = C_6H_{11}; X = Cl; Y = BF_4
8e: R = Ph; R' = $C_6H_3Me_2$-2,6; X = Cl; Y = CF_3SO_3
8f: R = Ph; R' = CMe_3; X = I; Y = CF_3SO_3
8g: R = Ph; R' = CMe_3; X = I; Y = BF_4

(3)

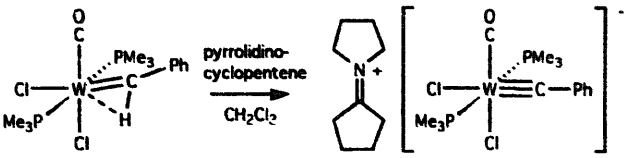

7c **9** (4)

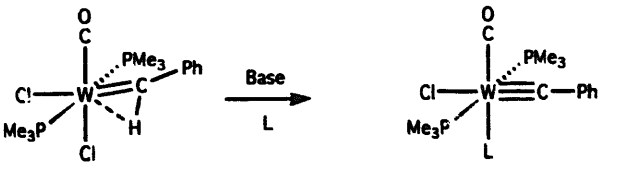

7c

4c: L = pyridine
5b: L = $CNCMe_3$
10: L = $P(OMe)_3$

(5)

The alkylidene hydrogen atoms of complexes **7** and **8** give rise to ^1H NMR signals in the range of $\delta -1.2$ to -3.4. The resonances are triplets due to coupling to the two phosphorus atoms of the PMe_3 ligands ($J_{PH} = 3$–4 Hz for **7** and 6–7 Hz for **8**). The signal for **7c** exhibits tungsten satellites, whereby $J_{WH} = 21.5$ Hz. The ^{13}C NMR resonances of the alkylidene carbon atoms of complexes **7** and **8** are found in the range of δ 220–240 as doublets of triplets due to coupling to the alkylidene hydrogen atom and the two phosphorus atoms ($J_{PC} \gg 11$ Hz). The C–H coupling constants range from 82 to 87 Hz for the neutral complexes **7** and from 67 to 77 Hz for the cationic complexes **8**. Very similar spectroscopic data have been reported for the related complex **7e** [15].

The protonation of the alkylidyne complexes can be reversed. Deprotonation of **7c** with 1-pyrrolidinocyclopentene affords the anionic alkylidyne complex **9** (Eq. (4)). The NMR parameters of **9** are normal for a Fischer-type alkylidyne complex [1]. One of the chloride ligands in **9** can be substituted by other ligands under very mild conditions. Thus deprotonation of **7c** with bases such as 1-pyrrolidinocyclopentene or n-BuLi, followed by the addition of pyridine, $CNCMe_3$, and $P(OMe)_3$ affords the alkylidyne complexes **4c**, **5b**, and **10**, respectively (Eq. (5)). Deprotonation of the cationic complexes **8** occurs very easily. For example, addition of triethylamine to **8b** immediately regenerates the alkylidyne complex **5b** (Scheme 2).

2.2. Crystallographic studies

The solid state structures of the complexes **5b**, **7a**, **7c**, and **8c** were determined by X-ray crystallography. The structure of **7a** was elucidated further by a neutron diffraction study. The crystal parameters and information on data collection and refinement are summarized in Table 1.

Selected bond distances and bond angles for **5b** are listed in Table 2. An ORTEP drawing of **5b** is shown in Fig. 1. The coordination sphere around tungsten is only slightly distorted from octahedral geometry. The alkylidyne ligand forms

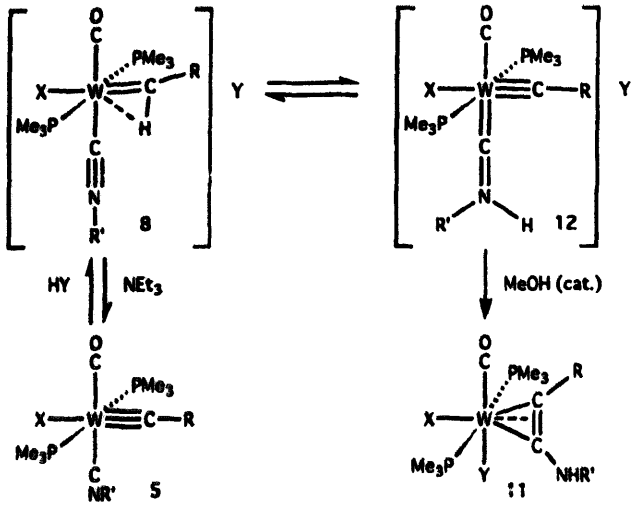

Scheme 2.

nearly perfect right angles with the carbonyl and the isocyanide ligands, and the chloride ligand is almost exactly opposite to the alkylidyne ligand. The trimethylphosphine ligands are bent away from the alkylidyne ligand by about 5°. They are also slightly bent towards the isocyanide ligand. The W–C(15) distance of 1.82(1) Å is normal for a tungsten–carbon triple bond [1] and the bond lengths between tungsten and the other ligands are also unexceptional. The alkylidyne ligand deviates very little from linearity.

Selected bond distances and bond angles for **7a** from the neutron diffraction study are given in Table 3. All geometric parameters are mutually consistent within the estimated standard deviations. The core of the molecular structure of **7a** is shown in Fig. 2. The coordination geometry can be described as distorted octahedral, if the η^2-alkylidene ligand is considered to occupy a single coordination site. The alkylidene carbon and hydrogen atoms, C(7) and H(1), have similar distances from the metal center, 1.857(4) and 1.922(6) Å, respectively. The C(7)–H(1) distance of 1.185(7) Å is significantly longer than a normal C(sp^2)–H bond [17]. The W(1)–C(7)–C(8) angle is 166.6(2)°, and the W(1)–C(7)–H(1) angle is 74.7(3)°. C(7) and H(1) are disposed on opposite sides of the axis defined by the extension of Cl(2)–W(1) bond. The Cl(2)–W(1)–C(7) and Cl(2)–W(1)–H(1) angles are 157.2(2) and 165.3(3)°, respectively. The C(7)Me group is proximal to the carbonyl ligand, and H(1) is proximal to Cl(1). The associated coordination angles C(7)–W(1)–C(9) and Cl(1)–W(1)–H(1) are small, 78.4(2) and 79.8(2)°, respectively. Perhaps as a consequence of these close contacts, the C(7)–H(1) bond is rotated from parallel alignment with the coordination axis containing the carbonyl ligand and Cl(1). As a consequence of this orientation, the alkylidene carbon atom is located atop the triangle defined by the atoms W(1), C(9), and P(2), and the C(9)–W(1)–P(2) angle is widened to 93.3(2) Å. The three ligands adjacent to the CMe fragment, namely the carbonyl and the two trimethylphosphine ligands, are bent towards the *trans*-chloride Cl(2). The bond angles Cl(2)–W(1)–L are 80.9(1), 86.3(1), and 81.0(1)° for L = C(9),

Table 1
Crystallographic data for the complexes **5b**, **7a** (neutron diffraction and X-ray diffraction), **7c**, and **8c**

Compound	**5b**	**7a** (neutron)	**7a** (X-ray)	**7c**	**8c**
Formula	$C_{10}H_{23}ClNOP_2W$	$C_9H_{23}Cl_2OP_2W$	$C_9H_{23}Cl_2OP_2W$	$C_{14}H_{24}C_{l_2}OP_2W$	$C_{16}H_{31}BClF_4NOP_2$
Fw	562.65	462.98	462.98	525.1	659.53
Space group	$P\bar{1}$ (No. 2)	$P2_1/c$ (No. 14)	$P2_1/c$ (No. 14)	$P2_1/n$ (No. 14)	$P2_1/n$ (No. 14)
a (Å)	11.5645(6)	11.838(5)	11.973(5)	8.420(2)	13.834(3)
b (Å)	11.6849(8)	11.103(8)	11.4967(9)	24.536(8)	17.057(7)
c (Å)	9.8517(6)	12.662(5)	12.8121(6)	9.719(2)	14.597(7)
α (°)	108.838(5)	90	90	90	90
β (°)	100.921(5)	102.89(4)	105.243(4)	104.90(2)	94.68(3)
γ (°)	89.095(5)	90	90	90	90
V (Å^3)	1235.7(3)	1622.3(15)	1702(1)	1940.3(9)	2747(3)
Z	2	4	4	4	4
T (K)	296	15	296	180	296
d(calc.) (g cm^{-3})	1.512	1.895	1.807	1.80	1.595
λ (Å)	0.71069	1.15863(8)	0.71069	0.71069	0.71069
Linear absorption coefficient (cm^{-1})	50.16	2.52	74.17	67.3	45.44
Scan mode	ω–2θ	ω–2θ	ω	ω	ω–2θ
2θ range (°)	2.8 < 2θ < 53.9	5.5 < 2θ < 108	2.8 < 2θ < 56.0	3 < 2θ < 50	2.8 < 2θ < 48.0
No. unique reflections	2806 [$I > 3\sigma(I)$]	3996	2700 [$I > 3\sigma(I)$]	2837 [$\|F_o\| > 3\sigma(F_o)$]	2749 [$I > 3\sigma(I)$]
Final no. variables	226	335	140	177	270
R	0.039 [a]	$R(F_o^2) = 0.157$ [c]	0.033 [a]	0.035 [a]	0.037 [a]
R_w	0.041 [b]	$R_w(F_o^2) = 0.141$ [d]	0.038 [b]	0.035 [b]	0.042 [b]
Goodness of fit	1.33	1.21	1.49	1.70	1.47

[a] $R = \Sigma\|\|F_o\| - \|F_c\|\|/\Sigma|F_o|$.
[b] $R_w = [\Sigma w(\|F_o\| - \|F_c\|)^2/\Sigma wF_o^2]^{1/2}$.
[c] $R(F_o^2) = \Sigma|F_o^2 - F_c^2|/\Sigma F_o^2$.
[d] $R_w(F_o^2) = [\Sigma w|F_o^2 - F_c^2|^2/\Sigma(wF_o^2)^2]^{1/2}$.

Table 2
Selected bond distances (Å) and angles (°) for **5b** and **8c**

5a		**8c**	
W(1)–Cl(1)	2.572(3)	W(1)–Cl(1)	2.449(3)
W(1)–P(1)	2.480(3)	W(1)–P(1)	2.520(3)
W(1)–P(2)	2.490(3)	W(1)–P(2)	2.513(3)
W(1)–C(10)	2.16(1)	W(1)–C(10)	2.17(1)
W(1)–C(15)	1.82(1)	W(1)–C(15)	1.88(1)
W(1)–C(16)	1.98(1)	W(1)–C(16)	2.03(1)
		W(1)–H(30)	1.88(8)
		C(15)–H(30)	1.17(8)
Cl(1)–W(1)–P(1)	85.94(9)	Cl(1)–W(1)–P(1)	80.4(1)
Cl(1)–W(1)–P(2)	83.43(9)	Cl(1)–W(1)–P(2)	83.5(1)
Cl(1)–W(1)–C(10)	90.4(3)	Cl(1)–W(1)–C(10)	91.9(3)
Cl(1)–W(1)–C(15)	179.2(3)	Cl(1)–W(1)–C(15)	161.5(3)
Cl(1)–W(1)–C(16)	90.7(3)	Cl(1)–W(1)–C(16)	83.4(3)
P(1)–W(1)–P(2)	168.64(9)	P(1)–W(1)–P(2)	163.1(1)
P(1)–W(1)–C(10)	89.8(3)	P(1)–W(1)–C(10)	83.6(3)
P(1)–W(1)–C(15)	94.9(3)	P(1)–W(1)–C(15)	90.8(3)
P(1)–W(1)–C(16)	91.3(3)	P(1)–W(1)–C(16)	95.4(3)
P(2)–W(1)–C(10)	86.3(3)	P(2)–W(1)–C(10)	91.8(3)
P(2)–W(1)–C(15)	95.7(3)	P(2)–W(1)–C(15)	106.1(3)
P(2)–W(1)–C(16)	92.8(3)	P(2)–W(1)–C(16)	87.9(3)
C(10)–W(1)–C(15)	89.7(4)	C(10)–W(1)–C(15)	103.3(4)
C(10)–W(1)–C(16)	178.5(4)	C(10)–W(1)–C(16)	175.3(4)
C(15)–W(1)–C(16)	89.2(4)	C(15)–W(1)–C(16)	81.3(4)
W(1)–C(15)–C(1)	179.3(8)	W(1)–C(15)–C(1)	167.8(8)
		W(1)–C(15)–H(30)	72(4)

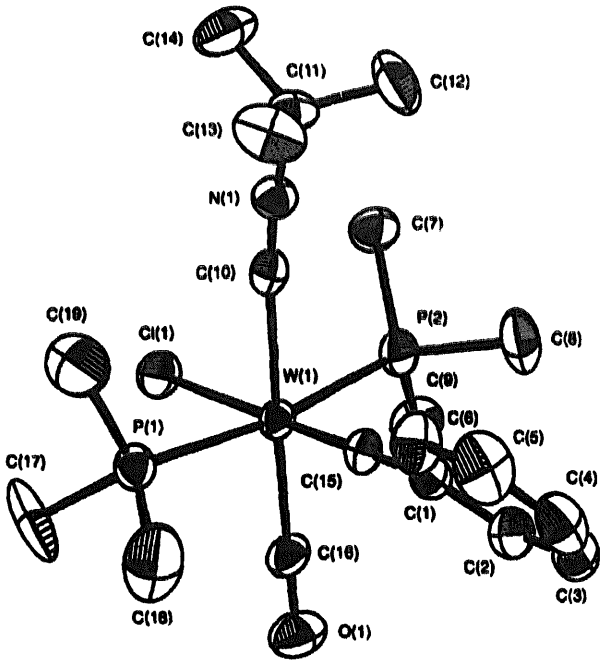

Fig. 1. Molecular structure of the alkylidyne complex **5b**.

P(1), and P(2), respectively. Cl(1), which is proximal to the alkylidene hydrogen atom, is not bent towards Cl(2). The Cl(1)–W(1)–Cl(2) angle is 90.9(1)°.

There is a short intermolecular contact of 2.554(6) Å between H(1) and Cl(1)′ of a neighboring molecule. Fig. 3 shows two perspectives of a pair of molecules connected by

Table 3
Selected bond distances (Å) and angles (°) for **7a** as determined by neutron diffraction

W(1)–Cl(1)	2.489(4)	W(1)–H(1)	1.922(6)
W(1)–Cl(2)	2.475(4)	C(7)–H(1)	1.185(7)
W(1)–P(1)	2.505(4)	C(8)–H(20)	1.109(8)
W(1)–P(2)	2.497(4)	C(8)–H(21)	1.096(8)
W(1)–C(7)	1.857(4)	C(8)–H(22)	1.079(8)
W(1)–C(9)	1.975(5)	Cl(1)–H(1)′	2.554(6)
Cl(1)–W(1)–Cl(2)	90.9(1)	Cl(2)–W(1)–H(1)	165.3(3)
Cl(1)–W(1)–P(1)	88.6(1)	P(1)–W(1)–P(2)	166.2(2)
Cl(1)–W(1)–P(2)	86.2(1)	P(1)–W(1)–C(7)	103.0(2)
Cl(1)–W(1)–C(7)	109.9(2)	P(1)–W(1)–C(9)	90.0(2)
Cl(1)–W(1)–C(9)	171.7(2)	P(2)–W(1)–C(7)	90.8(2)
Cl(1)–W(1)–H(1)	79.8(2)	P(2)–W(1)–C(9)	93.3(2)
Cl(2)–W(1)–P(1)	86.3(1)	C(7)–W(1)–C(9)	78.4(2)
Cl(2)–W(1)–P(2)	81.0(1)	W(1)–C(7)–C(8)	166.6(2)
Cl(2)–W(1)–C(7)	157.2(2)	W(1)–C(7)–H(1)	74.7(3)
Cl(2)–W(1)–C(9)	8[illegible](1)	C(8)–C(7)–H(1)	117.2(4)
Cl(1)–H(1)′–C(7)′	131.6(4)		

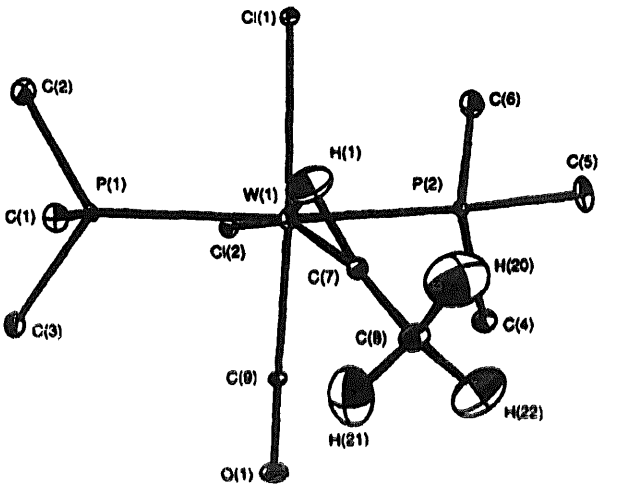

Fig. 2. ORTEP drawing of the molecular structure of the ethylidene complex **7a** as determined by neutron diffraction. The displacement ellipsoids of thermal motion are drawn at the 50% probability level. The hydrogen atoms of the trimethylphosphine ligands have been omitted for clarity.

two C(7)–H(1)···Cl(1)′ hydrogen bonds. As can be seen from Fig. 3(b), the oblique orientation of the C(7)–H(1) bond relative to the adjacent principal coordination axes is optimal as far as the intermolecular C(7)–H(1)···Cl(1)′ interaction is concerned. As a consequence of this orientation, the methyl group of the ethylidene ligand is in close contact with the $C(5)H_3$ group of the $P(2)Me_3$ ligand. The shortest H···H contact between $C(8)H_3$ and $C(5)H_3$ is 2.70 Å. The forces due to the intermolecular H(1)···Cl(1)′ attraction and the $C(8)H_3\cdots H_3C(5)$ repulsion may contribute to the slight, but discernible nonplanarity of the alkylidene ligand. The sum of the bond angles on C(7) is only 357.5(9)°.

The X-ray diffraction data for **7a** were collected at room temperature while the neutron diffraction data were measured at 15 K. Because of the temperature difference, the unit cell dimensions as determined by X-ray diffraction are noticeably

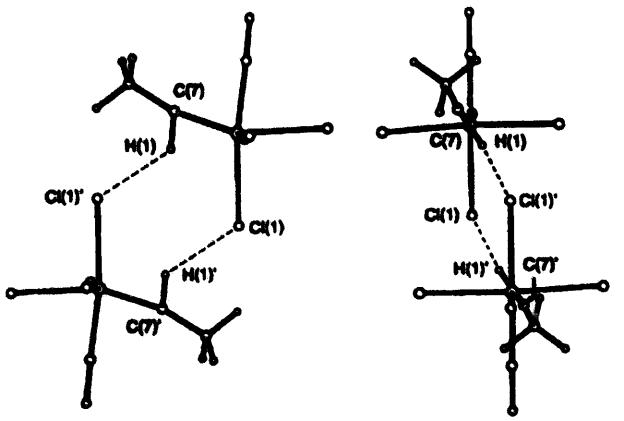

Fig. 3. Two views of a neighboring pair of molecules of **7a** showing the C(7)–H(1)···Cl(1)′ hydrogen bonding contacts.

Table 4
Selected bond distances (Å) and angles (°) for **7c**

W(1)–Cl(1)	2.444(2)	W(1)–C(7)	1.963(9)
W(1)–Cl(2)	2.480(2)	W(1)–C(8)	1.860(7)
W(1)–P(1)	2.511(3)	W(1)–H(8)	1.88
W(1)–P(2)	2.496(3)		
Cl(1)–W(1)–Cl(2)	91.6(1)	P(1)–W(1)–P(2)	171.3(1)
Cl(1)–W(1)–P(1)	89.1(1)	P(1)–W(1)–C(7)	87.9(3)
Cl(1)–W(1)–P(2)	84.5(1)	P(1)–W(1)–C(8)	100.4(3)
Cl(1)–W(1)–C(7)	77.7(2)	P(2)–W(1)–C(7)	96.5(3)
Cl(1)–W(1)–C(8)	154.5(2)	P(2)–W(1)–C(8)	87.8(3)
Cl(2)–W(1)–P(1)	89.1(1)	C(7)–W(1)–C(8)	79.1(3)
Cl(2)–W(1)–P(2)	85.3(1)	W(1)–C(8)–C(9)	164.6(6)
Cl(2)–W(1)–C(7)	168.9(2)	W(1)–C(8)–H(8)	74.6
Cl(2)–W(1)–C(8)	111.9(2)	C(9)–C(8)–H(8)	120.8

larger than those obtained by neutron diffraction (Table 1). Nevertheless, the intramolecular bond distances, except those involving hydrogen atoms, are nearly identical within the error limits, and are therefore not listed in the Tables. Where small differences exist, the neutron values are slightly larger than the X-ray values, reflecting a small systematic foreshortening from the larger atomic displacement parameters at room temperature. The X-ray structure of the analogous neopentylidene complex **7e** was determined by Churchill and Wasserman [18]. The structural features of **7e** are very similar to those of **7a**.

Selected bond distances and bond angles for compound **7c** are given in Table 4, and the molecular structure is shown in Fig. 4. The distance between tungsten and the alkylidene carbon atom, W–C(8), is 1.860(7) Å, and the separation between tungsten and the alkylidene hydrogen atom, W–H(8), is 1.88 Å. In the crystal, the molecules are packed in pair-wise fashion similar to the crystal structure of **7a**, but presumably due to the larger size of the alkylidene substituent (phenyl versus methyl), the intermolecular C(8)–H(8)··· Cl(2) interaction is significantly longer (about 3.1 Å).

Selected bond distances and bond angles for **8c** are listed in Table 2. The molecular structure of the cation of **8c** is

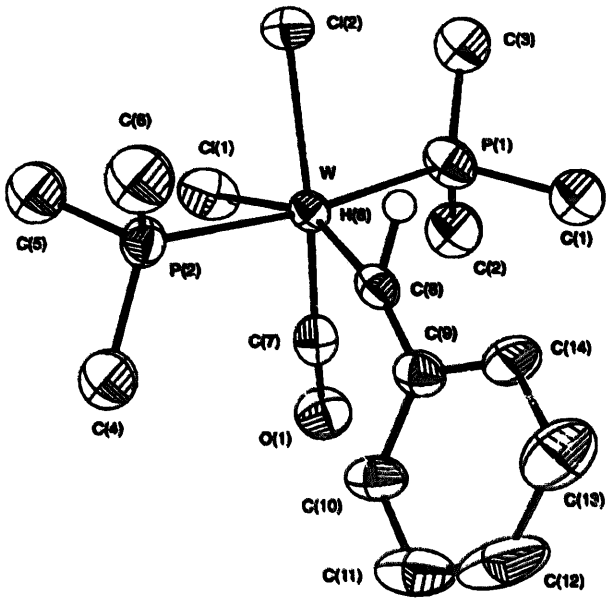

Fig. 4. ORTEP drawing of the molecular structure of **7c**.

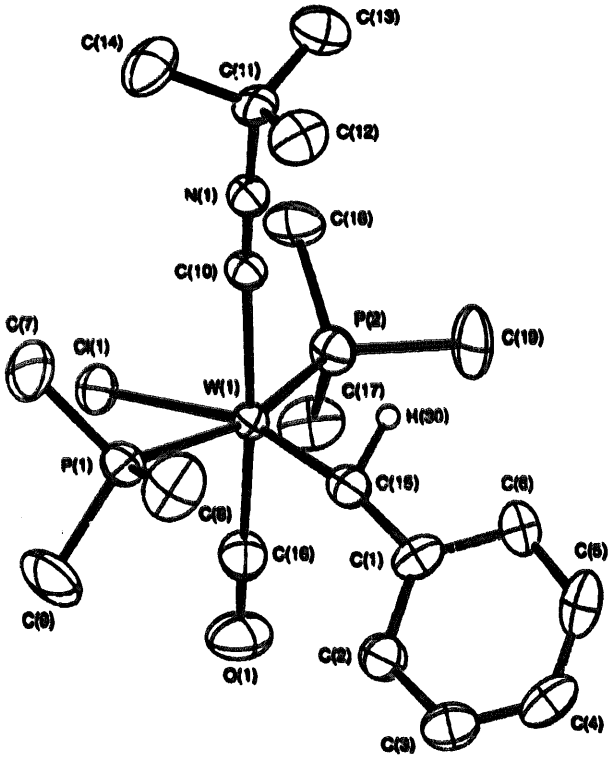

Fig. 5. ORTEP drawing of the molecular structure of the cation of **8c**.

shown in Fig. 5. Complex **8c** is structurally very similar to the neutral alkylidene complexes **7a** and **7c**. The C(15)–H(30) bond is oriented towards the location of the BF_4^- counterion (not shown in Fig. 5), presumably as a result of electrostatic interactions, but even the shortest distances between H(30) and the (disordered) fluorine atoms of about 2.3 Å are too long to indicate the presence of hydrogen bonding contacts of significant strength.

3. Discussion

3.1. Protonation of the tungsten alkylidyne complexes and deprotonation of the tungsten alkylidene complexes

The protonation reactions of the alkylidyne complexes $[W(CR)Cl(CO)L(PMe_3)_2]$ (**3** (L = PMe_3) and **4** (L = py), by HCl (Eq. (2)) are accompanied by the loss of the ligand L. This transformation may be reversed. Deprotonation of complex **7c** in the presence of ligands L′ affords alkylidyne complexes of the type $[W(CPh)Cl(CO)L'(PMe_3)_2]$ (Eq. (5)). This is a useful procedure, indeed one of the mildest to introduce new ligands into alkylidyne metal complexes.

Protonation of the isocyanide-substituted alkylidyne complexes **5** with HCl does not result in the formation of isolable alkylidene complexes; instead, aminoalkyne complexes of the type $WCl_2(RCCNHR')(CO)(PMe_3)_2$ and nitrilium (iminoacyl) complexes of the type $[W(RCH_2CNR')Cl_3(CO)(PMe_3)]$ are obtained [19]. The cationic alkylidene complexes **8**, however, can be isolated, if the 'non-nucleophilic' acids HBF_4 and $HOSO_2CF_3$ are used. In the presence of small amounts of methanol or water, the alkylidene complexes **8** isomerize into aminoalkyne complexes of type **11** (Scheme 2) [10]. A kinetic investigation of this isomerization revealed that a small concentration of the N(isocyanide)-protonated isomers **12** exists in equilibrium with the C(alkylidyne)-protonated complexes **8**. Thus the alkylidyne tungsten isocyanide complexes **5** feature at least two sites at which protonation may occur. The equilibrium in Scheme 2 implies reversibility of the protonation steps. Indeed, even moderately strong bases such as triethylamine cause the immediate deprotonation of complexes **8** and regeneration of the alkylidyne complexes **5** (Scheme 2). The weakness of the alkylidene C–H bonds is also reflected in the low carbon–hydrogen coupling constants [16]. The J_{CH} values for the cationic complexes **8**, which range from 67 to 77 Hz, are lower by about 10 Hz than the values for the neutral complexes **7**. In accordance, the cationic complexes **8** are significantly more easily deprotonated than the neutral complexes **7**.

There is no evidence for protonation at the metal center of the alkylidyne complexes **3–5**, which, in principle, should be feasible. In general, the outcome of protonation reactions of alkylidyne metal complexes depends strongly on the nature of the ancillary ligands. For example, protonation of $[W(CCMe_3)Cl(PMe_3)_4]$ with $HOSO_2CF_3$ affords the alkylidene complex **13**, while protonation of the sterically less congested complex $[W(CCMe_3)Cl(dmpe)_2]$ (dmpe = bis-dimethylphospinoethane) gives the alkylidyne hydrido tungsten complex $[W(CCMe_3)(Cl)(H)(dmpe)_2][SO_3CF_3]$ [8a–c]. Equilibria between alkylidene and alkylidyne hydrido metal complexes have been observed for electronically related tantalum complexes such as $[Ta(CHCMe_3)I(dmpe)_2]$ and $[Ta(CCMe_3)(H)I(dmpe)_2]$ [8d]. In the case of $[Mo(CCH_2CMe_3)(\eta^5\text{-}C_5H_5)\{P(OMe)_3\}_2]$, there is evidence that the initial protonation product is $[Mo(CHCH_2CMe_3)(\eta^5\text{-}C_5H_5)\{P(OMe)_3\}_2]^+$ [8d–e]. In this system, the alkylidene complex rearranges into the alkylidyne hydrido complex $[Mo(CCH_2CMe_3)(\eta^5\text{-}C_5H_5)(H)\{P(OMe)_3\}_2]^+$, if the counterion is non-coordinative. The available results suggest that the alkylidyne carbon atom is generally the preferred site of initial proton addition. This is in agreement with theoretical calculations according to which the alkylidyne carbon atom is carrying a net negative charge [20]. However, in the absence of strong π acceptor ligands or steric crowding of the metal center, the alkylidene metal complexes rearrange into alkylidyne hydrido metal complexes [21]. Several other stable alkylidene metal complexes containing good π acceptor ligands are the ethylene tungsten complex **14** [16], the alkyne tungsten complex **15** [22], and the ethylene tantalum complex **16** [23]. Related alkylidyne hydrido/alkylidene metal complex pairs have been observed with $[Os(CR)Cl_2H(PR'_3)_2]$ [24] and $[Ru(CHR)Cl_2(PR'_3)_2]$ [25]. The interconversion of the iridium alkylidyne and vinylidene hydrido species $[Ir(CCH_2R)Cl(PR_3)_2]$ and $[Ir(CCHR)ClH(PR_3)_2]$ is also of interest in this context [26].

In the alkylidene alkyne tungsten complexes **15**, the C–H bond is only weakly interacting with the metal center, since the electron deficiency of the metal center is alleviated by electron π donation from the alkyne ligand [22]. Electronically saturated alkylidene metal complexes have also been obtained in protonation reactions of other alkylidyne metal complexes where the metal can interact with an internal donor site. Thus protonation with HBF_4 of thiocarbyne metal complexes, such as $[W(CSMe)(tris\text{-}pyrazolylborate)(CO)_2]$, affords complexes of the type $[W(\eta^2\text{-}CHSMe)(tris\text{-}pyrazolylborate)(CO)_2][BF_4]$. In these compounds the η^2-methylthiomethylidene ligand is coordinated to the metal center via the carbon atom and the sulfur atom, not the hydrogen atom [7b,c]. Addition of acids HX across metal–carbon triple bonds has been observed in a variety of systems where an expansion of the coordination sphere is feasible. Thus, reaction of HX with $[W(CTol)(\eta^5\text{-}C_5H_5)(CO)_2]$ (Tol = C_6H_5Me-4) or $[Cr(CNEt_2)(\eta^5\text{-}C_5H_5)(CO)_2]$ yields the electronically saturated alkylidene complexes $[W(CHTol)(\eta^5\text{-}C_5H_5)I(CO)_2]$ [3] (X = I) and $[Cr(CHNEt_2)(\eta^5\text{-}C_5H_5)Cl(CO)_2]$ (X = Cl) [7a]. Similarly, addition of HCl across the metal–carbon triple bond in the trigonal bipyramidal Roper-type alkylidyne complexes affords octahedral alkylidene complexes of the type $[Os(CHTol)Cl_2(CO)(PPh_3)_2]$ [1f,27]. On the other hand, addition of HX (X = Cl, Br, O_2CR, OAr) across the metal–carbon triple bond in electronically unsaturated Schrock-type alkylidyne complexes of the type $[W(CCMe_3)(OCMe_3)_3]$ affords agostic [28] alkylidene complexes such as $[W(CHCMe_3)X_2(OCMe_3)_2]$ [1e,29]. As is the case for compounds **7** and **8**, several of these protonation reactions have been demonstrated to be reversed by the addition of base.

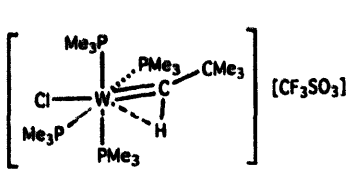

13

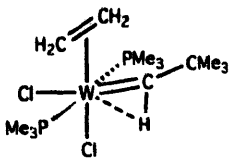

14

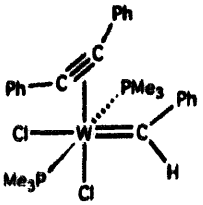

15

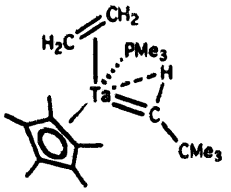

16

3.2. Solid state structures of the alkylidyne and alkylidene complexes

Fig. 6 shows two views of the superimpositions of the core of the neutron structure of **7a** with those of the X-ray structures of **7c**, and **8c**. These drawings illustrate the similarity of the alkylidene complexes **7** and **8** and highlight the important common structural features: (1) The alkylidene carbon and hydrogen atoms are approximately equidistant from the metal center. The C–H bond, *not* the alkylidene carbon atom, may be considered to occupy the 'octahedral coordination site'. The W–C–C angle on the alkylidene ligand is wide, ranging from 164 to 168°. (2) The alkylidene carbon atom is proximal to the carbonyl ligand. (3) Relative to the four *cis* ligands, the C–H bond adopts roughly a half-diagonal orientation. The two ligands closest to the CR group, the carbonyl and one of the two trimethylphospine ligands, are strongly bent towards the *trans*-chloride ligand (Cl–W–CO, 78–82°; Cl–W–P, 80–85°). The associated OC–W–P angles are relatively wide, ranging from 93 to 97°. The second PMe_3 ligand is also pushed towards the *trans* chloride ligand, but to a smaller extent (Cl–W–P, 84–89°). The ligand proximal to the hydrogen atom, i.e. Cl in **7** and $CNCMe_3$ in **8**, is not pushed towards the *trans* chloride ligand (Cl–W–L, 90–92°).

The availability of the structures of the alkylidyne complex **5b** and its protonated form **8c** offers a unique opportunity to determine the precise structural changes accompanying the protonation of an alkylidyne complex. Corresponding geometric parameters of **5b** and **8c** are juxtaposed in Table 2. Three perspectives of the superimposed structures of **5a** and **8c** are shown in Fig. 7. Not surprisingly, the CPh group is the part of the molecule most strongly affected by the addition of the proton. The tungsten–carbon distance increases from 1.82(1) to 1.88(1) Å, and the W–C–C(Ph) group bends by about 12°. The most striking change, however, is the 'lateral' shift of the CPh group away from the coordination axis defined by the extension of the Cl(1)–W(1) bond. This change is clearly discernible in all three perspectives of Fig. 7. The lateral shift of C(15) is approximately 0.6 Å, as meas-

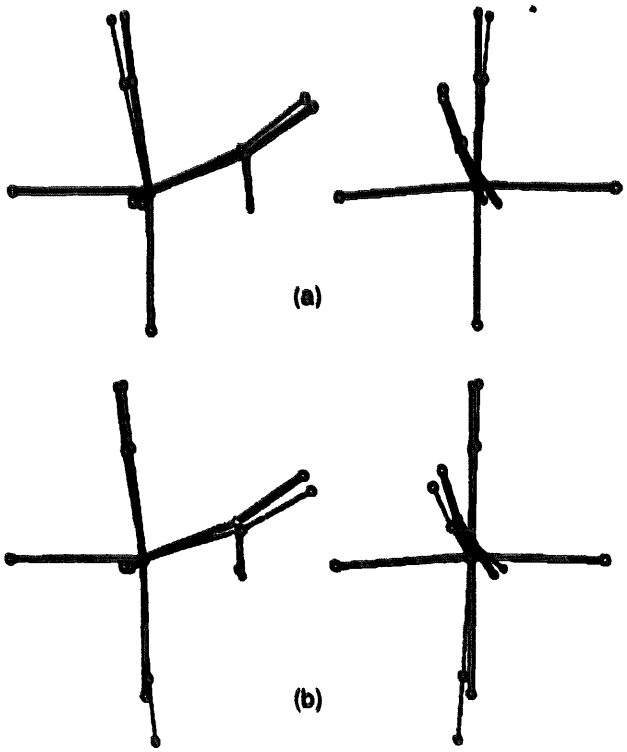

Fig. 6. Perspective views along major coordination axes of the superimpositions of the neutron structure of **7a** (double lines) and the X-ray structures (single lines) of (a) **7c** and (b) **8c**. Only the structural cores are shown. In the superimpositions, mirror images of the structures of **7c** and **8c** have been used to obtain the same orientations of the alkylidene ligands.

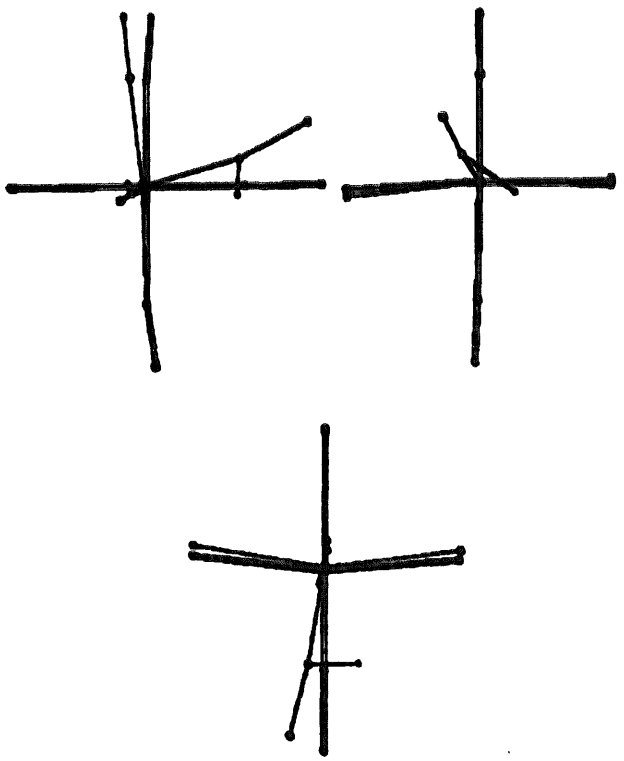

Fig. 7. Three views along the principal coordination axes of the superimposed core structures of the benzylidyne complex **5b** (double lines) and the benzylidene complex **8c** (single lines).

ured by the separation of the alkylidyne and alkylidene carbon atoms in the superimposed structures. Instead of C(15), the newly formed C–H bond may be considered to occupy the 'octahedral coordination site'. The CPh group is shifted towards the carbonyl ligand, not directly, but with a slant towards one of the trimethylphosphine ligands, P(1)Me_3. As a consequence, the CO and P(1)Me_3 ligands are strongly pushed towards the *trans* chloride ligand, by 7.3 and 5.5°, respectively, and the C(16)–W–P(1) angle widens by approximately 4°. The two ligands nearest to the alkylidene hydrogen atom, the isocyanide and P(2)Me_3, are affected to a much smaller extent. The protonation of the alkylidyne ligand causes the bond between the metal and the trans chloride ligand, W(1)–Cl(1), to contract from 2.572(3) to 2.449(3) Å. This shortening of the W–Cl bond may be ascribed to a smaller trans influence [30] of the alkylidene ligand compared with that of the alkylidyne ligand. The bond contraction is probably amplified by the overall positive charge of **8c**, but this influence may be tempered by increased steric crowding due to the 'bending back' of the carbonyl and PMe_3 ligands.

The neutron structure of the electronically related tantalum neopentylidene complex **16** has been reported by Schultz et al. [23]. As is the case for complexes **7** and **8**, complex **16** is a d^2 system, considering the alkylidene ligand as a dianion. The geometric parameters of the alkylidene ligand of **16** are similar to those found in complexes **7** and **8**. The alkylidene C–H bond length is 1.135(3) Å, the Ta–H separation is 2.042(5) Å, and the Ta–C(alkylidene) distance is 1.946(3) Å. The structural parameters of d^0 alkylidene complexes are qualitatively different [31]. In general, the M–C(alkylidene) distance is distinctly shorter than the M–H distance and the M–C(H)–R bond angles are smaller than those found in the d^2 systems. The structure of $[Ta(CHCMe_3)(PMe_3)Cl_3]_2$, which has also been determined in a neutron diffraction study [23] may serve as a typical example for this class of alkylidene complex. In this compound, the Ta–C(alkylidene) bond length is 1.898(2) Å while the Ta–H distance is 2.119(4) Å. The Ta–C(H)–CMe_3 angle is 161.2(1)°.

A feature of special interest in the solid-state structure of **7a** is the presence of the intermolecular hydrogen bonds between the activated C–H bonds and chloride ligands of neighboring molecules. The H(1)···Cl(1)′ distance of 2.554(6) Å is significantly shorter than the sum of the van der Waals radii of hydrogen (1.20 Å) and chlorine (1.75 Å) [17] and similar in length to a number of C–H···Cl hydrogen bonds reported in the literature [32]. However, a more relevant precedent may be the intermolecular hydrogen bond in the solid state structure of $[IrCl_2H(H_2)(P\text{-}i\text{-}Pr_3)_2]$ between a hydrogen atom of the η^2-dihydrogen ligand and a chloride ligand on a neighboring molecule [33]. The IrH–H···Cl′Ir′ distance in this structure is 2.64(2) Å, which is slightly longer than the contact in **7a**. Thus the intermolecular hydrogen bonds of **7a** may well be slightly stronger than those of the iridium system. Nevertheless, on an absolute scale, the hydrogen bonds of **7a** are probably quite weak and possibly not even a major factor in determining the pairwise arrangement of the molecules in the crystal packing of **7a**. We note that in the crystal structure of **7c**, the molecules are packed in the same pairwise fashion as in **7a**, even though the intermolecular C–H···Cl′ contacts are about 3.1 Å, which is longer than the sum of the van der Waals radii.

3.3. Structures of electronically related complexes

Several tungsten alkylidene complexes reported in the literature share some of the characteristic structural features of complexes **7** and **8**. Templeton and coworkers reported the structure of $[W(CCH_3Ph)(Tp')(CO)_2][BF_4]$ (Tp′ = hydridotris(3,5-dimethylpyrazolyl)borate) (**17**) [34]. The vinylcarbene complex **18** was studied in our laboratory [35]. In these two types of compounds, the alkylidene carbon atom and a second intraligand donor site located on the β-carbon atom, namely a β-CH bond and a β,γ-unsaturation, respectively, are interacting with the metal center. The M–C–C(Ph) angles in **17** and **18** (149(2) and 147.9(7)°, respectively) are also distorted, but to a smaller extent than in the α-agostic complexes **7** and **8**, because the β-substituents can reach the metal center more easily. As in **7** and **8**, the alkylidene carbon atoms are shifted towards the carbonyl ligands (PhC–W–CO, 75.6(4) and 76.9(4)° in **18**).

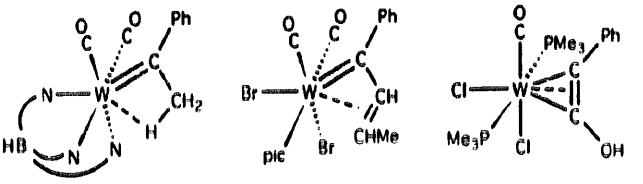

17 18 19

Less obvious relatives of the α-agostic metal alkylidenes are complexes of four electron donor alkyne ligands [36]. Several of these have the same metal complex fragment as the complexes **7**. Of particular interest is the structurally characterized complex $[W(PhCCOH)Cl_2(CO)(PMe_3)_2]$ (**19**) [37]. This compound can formally be derived from $[W(PhCH)Cl_2(CO)(PMe_3)_2]$ (**7c**) by substituting a COH group for the alkylidene hydrogen atom. The structural similarities between **7c** and **19** are striking. In fact, except for the region directly affected by the modification, the two structures are almost identical. This is evident from the three perspectives of the superimposition of **7c** and **19** shown in Fig. 8. The large W–C–Ph angle of the alkylidene ligand in **7c** (165°) is comparable to that of the corresponding W–C–Ph group in **19** (156°), and the OC–W–C(Ph) angles in **7c** and **19** differ by less than 3°. The W–CPh distance of 2.05(1) Å in **19**, although approximately 0.2 Å longer than the W–CPh distance in **7c**, is still within the range of tungsten–carbon double bonds [38]. The alkylidene C–H and the alkyne C–C axes are rotated from alignment with the metal–carbonyl axis by almost the same amount. The three ligands adjacent to the CPh group are pushed towards the trans chlo-

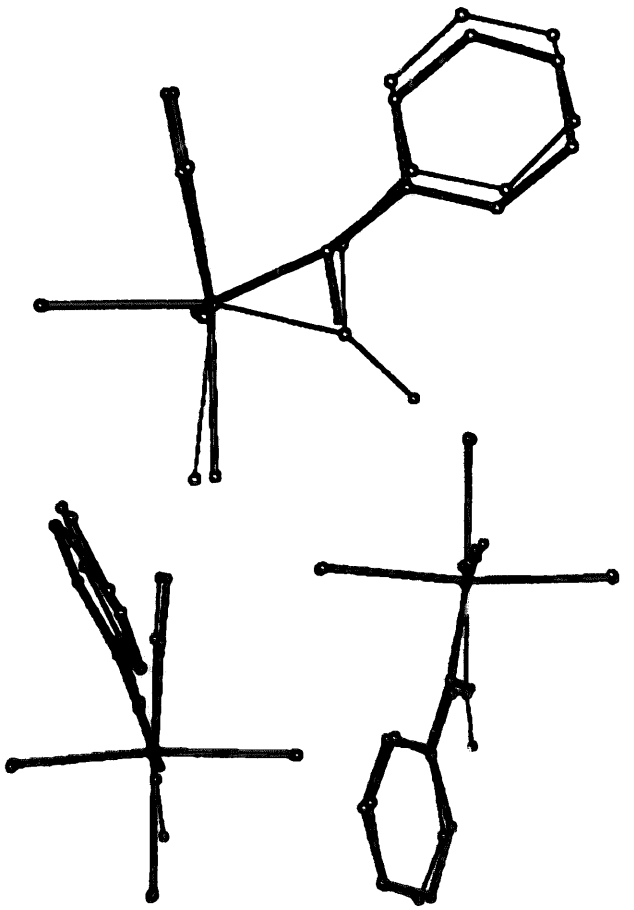

Fig. 8. Three views along the principal coordination axes of the superimposed core structures of [W(CHPh)Cl_2(CO)(PMe_3)$_2$] (**7c**) (double lines) and [W(CPhCOH)Cl_2(CO)(PMe_3)$_2$] (**19**) (single lines).

ride ligand very nearly to the same extent in both complexes, but the *cis* chloride, which experiences little steric pressure from the alkylidene hydrogen atom in **7c**, is also strongly bent towards the *trans* chloride in **19**, owing to the larger influence of the COH group.

3.4. Qualitative bonding considerations

α-Agostic alkylidene metal complexes, including compounds of the type discussed here, have been the subject of a theoretical study by Hoffmann and coworkers [39]. The bonding between the metal center and the alkylidene ligand can be described as a triple bond. The C–H σ orbital acts as the σ donor towards the metal center. This is in agreement with the finding that the C–H bond occupies the 'octahedral coordination site'. Two metal–ligand π interactions involve the p and 'sp^2' orbitals of the CHR fragment. The alkylidene σ* orbital is significantly higher in energy than the σ, p, and 'sp^2' orbitals and probably is contributing little to the metal–alkylidene interaction. An analogy can be drawn between the trio of metal–alkylidene bonds and the bonding of four-electron donor alkyne ligands or ketenyl ligands [36,40]. As in the case of ketenyl ligands, the orientation of the alkylidene ligand relative to the adjacent ligands is influenced by the asymmetry of a metal–ligand π bond. In the electronically preferred orientation of the alkylidene ligand, the large lobe of the 'sp^2' orbital is oriented towards the carbonyl π* orbital.

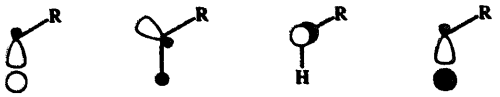

σ 'sp^2' p σ*

The d^2 alkylidene metal complexes containing strong π acceptor ligands, i.e. complexes **7**, **8**, **13**, **14**, and **15**, do not rearrange into alkylidyne hydrido metal complexes by migration of the hydrogen atom (proton) from the alkylidene carbon atom to the metal center. The formation of a localized M–H bond would eliminate the π backbonding from the metal center to the π acceptor ligands (formal oxidation of the metal from d^2 to d^0) and consequently entail the loss of these ligands. This step would only further increase the unsaturation of the metal center. Thus the π acceptor ligands are 'arresting' the migration of the hydrogen atom from the alkylidene carbon atom to the metal center which would undoubtedly occur in their absence.

The behavior of the side-on bonded C–H bond is not unlike that observed for metal-coordinated dihydrogen. Just as the C–H bond is more easily deprotonated in the cationic complexes **8** than in the neutral complexes **7**, so is heterolytic cleavage of H_2 promoted by more strongly electrophilic metal centers [41]. On the other hand, the oxidative addition of the H–H bond can also be suppressed by the presence of strong π acceptor ligands [42].

4. Concluding remarks

Protonation of alkylidyne carbonyltungsten complexes affords η^2-alkylidene carbonyltungsten complexes. The C–H bonds of the alkylidene ligands are easily deprotonated, but in contrast to the protonation products of Fischer-type alkylidyne metal complexes containing no or only weak π acceptor ligands, the alkylidene carbonyl tungsten complexes do not rearrange into alkylidyne hydrido tungsten systems. The protonation of the alkylidyne ligand causes a lengthening of the W–CR distance and induces a lateral shift of the CR group, apparently in order to optimize the interaction between the metal center and the newly formed C–H bond. The remaining structural changes are primarily a consequence of the larger steric demand and the smaller *trans* influence of the η^2-alkylidene ligand compared with the alkylidyne ligand. The interaction between the metal center and the agostic C–H bonds is strong, whereby the W–C and W–H distances are of almost equal length, and the C–H bond lengths are significantly longer than those of normal C–H bonds. A striking structural and electronic similarity exists between η^2-alkylidene and 4-electron donor alkyne metal complexes.

5. Experimental

Standard inert-atmosphere techniques were used in the synthesis of the compounds. The solvents methylene chloride (CaH_2), hexane (CaH_2), THF, and ether (Na/benzophenone) were dried and distilled prior to use. The pentacarbonyltungsten acyl complexes were prepared as described by Fischer and Maasböl [11a]. Complexes **1a**, **1c**, **2c**, and **3c** were prepared based on literature procedures [12,13]. The NMR spectra were measured at 250 or 300 MHz (for ^{1}H NMR) in $CDCl_3$ at room temperature unless otherwise noted; solvent peaks were used as internal reference, and the chemical shifts are reported in δ relative to TMS. Elemental analyses were performed by Schwarzkopf Microanalytical Laboratory and M-H-W Laboratories.

5.1. Syntheses

5.1.1. [W(CEt)Cl(py)$_2$(CO)$_2$] (1b)

[NMe_4][W{C(O)Et}$(CO)_5$] (7.90 g, 17.37 mmol) is dissolved in methylene chloride (100 ml), and the solution is cooled to −78°C. A pre-cooled (−78°C) solution of oxalyl chloride (1.50 ml, 17.20 mmol, 1 equiv.) in methylene chloride (40 ml) is added to it. The color of the solution changes from light yellow to dark orange. The mixture is stirred at −78°C for 5 min, the bath is then removed and the solution allowed to warm slowly until it turns yellow (−10°C). Pyridine (15 ml) is added and the mixture stirred at room temperature until the reaction is complete (1 h). During this time, the color of the solution changes from yellow to brown. The solvent is removed in vacuo, and the product is washed with hexane (2×10 ml). The product is purified by column chromatography at −30°C (SiO_2 and CH_2Cl_2/hexane, 1:1). The product is obtained as light yellow crystals after recrystallization from CH_2Cl_2/hexane (2.738 g, 33.5%). IR (CH_2Cl_2, cm^{-1}): ν(CO) = 1983 (s), 1892 (s). ^{1}H NMR: δ 1.23 (t, J = 7.5 Hz, 3H, CH_2CH_3), 2.63 (q, J = 7.5 Hz, 2H, CH_2CH_3), 7.3 (m, 4H, β-py), 7.8 (m, 2H, γ-py), 9.0 (m, 4H, α-py). ^{13}C NMR: δ 11.4 (CH_2CH_3), 42.0 (J_{WC} = 38.6 Hz, CH_2CH_3), 124.6, 138.0, 152.4 (py), 220.2 (J_{WC} = 170 Hz, CO), 281.1 (J_{WC} = 195 Hz, W≡C).

5.1.2. [W(CC$_6$H$_4$Me-4)Cl(py)$_2$(CO)$_2$] (1d)

[NMe_4][W{C(O)(C_6H_4Me-4)}$(CO)_5$] (2.1 g, 4.06 mmol) is dissolved in methylene chloride (400 ml), and the solution is cooled to −78°C. A pre-cooled (−78°C) solution of oxalyl chloride (0.52 g) in methylene chloride (30 ml) is added. The color of the solution changes from light orange to dark red. The cold bath is removed, and the solution is allowed to warm slowly to 0°C. Pyridine (1.6 g) is added, and the mixture stirred at room temperature until the reaction is complete (2 h). The solution is filtered through a plug of silica (2×2 cm). The solvent is removed in vacuo, and the product is washed with hexane (2×15 ml). Recrystallization from CH_2Cl_2/pentane gives a yellow powder. (1.16 g, 53%). IR (CH_2Cl_2, cm^{-1}): ν(CO) = 1980 (s), 1909 (s). ^{1}H NMR: δ 3.8 (s, 3H, CH_3), 6.8–7.3 (m, 8H, C_6H_4, β-py), 7.8 (2H, γ-py), 9.1 (4H, α-py). ^{13}C NMR: δ 55.4 (CH_3), 113.1, 125.1, 131.0, 138.3, 142.1, 152.5, 158.7 (C_6H_4, py), 220.7 (CO), 263.7 (W≡C).

5.1.3. [W(CC$_6$H$_4$NMe$_2$-4)Cl(py)$_2$(CO)$_2$] (1e)

1e is prepared by reaction of [NMe_4][W{C(O)-($C_6H_4NMe_2$-4}$(CO)_5$] (8.557 g, 15.70 mmol) with oxalyl chloride (1.20 ml, 13.76 mmol) following the procedure described for **1b** and purified by column chromatography at −20°C (SiO_2, CH_2Cl_2/hexane, 2:1). Orange crystals from CH_2Cl_2/hexane (6.89 g, 89.0%). IR (CH_2Cl_2, cm^{-1}): ν(CO) = 1976 (s), 1889 (s). ^{1}H NMR: δ 3.04 (s, 6H, Me_2N), 6.6–7.4 (m, 8H, C_6H_4, β-py), 7.8 (2H, γ-py), 9.2 (4H, α-py). ^{13}C NMR: δ 39.8 (Me_2N), 110.9, 124.9, 130.8, 138.2, 149.8, 152.65 (C_6H_4, py), 221.9 (J_{WC} = 172 Hz, CO), 266.7 (W≡C).

5.1.4. cis-[W(CMe)Cl(CO)$_2$(PMe$_3$)$_2$] (2a)

1a (4.884 g, 1.06 mmol) is dissolved in methylene chloride (70 ml) and PMe_3 (2.10 ml, 2.03 mmol) is added. The mixture is stirred at room temperature until the reaction is complete (1 h). During this time the color of the solution changes from yellow to dark orange. The solvent is removed in vacuo, and the mixture is washed with hexane (2×10 ml). The product is purified by column chromatography at −40°C (SiO_2, CH_2Cl_2/hexane, 1:1). The product is obtained as yellow crystals after recrystallization from toluene/hexane (3.20 g, 70%). IR (KBr, cm^{-1}): ν(CO) = 1986 (s), 1906 (s). ^{1}H NMR: δ 1.87 (t, $^2J_{PH}$ = 4.2 Hz, 3H, CCH_3), 1.60 (d, 18H, PMe_3). ^{13}C NMR: δ 18.5 (t, J_{CP} = 14 Hz, PMe_3), 36.6 (CCH_3), 212.2 (t, J_{PC} = 18 Hz, CO), 276.9 (t, J_{PC} = 10.5 Hz, W≡C). ^{31}P NMR: δ −27.5 (J_{WP} = 240 Hz). *Anal.* Calc. for $WC_{10}H_{21}ClO_2P_2$ (0.1 toluene): C, 27.71; H, 4.74. Found: C, 27.98; H, 5.04%.

5.1.5. cis-[W(CEt)Cl(CO)$_2$(PMe$_3$)$_2$] (2b)

1b (0.734 g, 1.55 mmol) is treated with PMe_3 (300 ml, 2.95 mmol) for 30 min, following the procedure described for **2a**. Column chromatography at −40°C (SiO_2, first eluted with CH_2Cl_2/hexane, 2:1, then CH_2Cl_2/THF, 98:2). The product is obtained as light yellow crystals after recrystallization from ether/hexane (0.583 g, 81%). IR (CH_2Cl_2, cm^{-1}): ν(CO) = 1998 (s), 1920 (s). ^{1}H NMR: δ 1.0 (t, 3H, CH_2CH_3), 1.6 (d, 18H, PMe_3), 2.08 (m, 2H, CH_2CH_3). ^{13}C NMR: δ 11.6 (CH_2CH_3), 18.1 (t, J_{PC} = 13.9 Hz, PMe_3), 42.9 (CH_2CH_3), 212 (m, CO), 284.2 (t, J_{PC} = 10 Hz, W≡C). ^{31}P NMR: δ −25.5 (J_{WP} = 242 Hz).

5.1.6. cis-[W(CC$_6$H$_4$CH$_3$-4)Cl(CO)$_2$(PMe$_3$)$_2$] (2d)

1d is dissolved in methylene chloride, and PMe_3 (two equivalents) is added. The mixture is stirred at room temperature for 2 hours. The volatile components are removed under vacuum, and the residue is washed several times with cold hexane (0°C). IR (CH_2Cl_2, cm^{-1}): ν(CO) = 1987 (s),

1917 (s). The product was used in the preparation of **3d** without further characterization.

5.1.7. *cis*-[W(CC$_6$H$_4$NMe$_2$-4)Cl(CO)$_2$(PMe$_3$)$_2$] (2e)

1e (2.986 g, 5.28 mmol) is treated with PMe_3 (1.060 ml, 10.24 mmol), following the procedure described for **2a**. Light orange crystals from CH_2Cl_2/ether/hexane (2.56 g, 88 0%). IR (CH_2Cl_2, cm^{-1}): ν(CO) = 1990 (s), 1916 (s). ^{1}H NMR: δ 1.63 (d, 18H, PMe_3), 2.95 (s, 6H, Me_2N), 6.45–7.10 (m, 4H, C_6H_4). ^{13}C NMR: δ 18.8 (m, PMe_3), 39.7 (Me_2N), 110.5, 130.5, 138.5, 149.12 (C_6H_4), 212.7 (m, CO), 270.1 (J_{PC} = 11 Hz, W≡*C*). ^{31}P NMR: δ −25.8 (J_{WP} = 260 Hz, PMe_3).

5.1.8. [W(CMe)Cl(CO)(PMe$_3$)$_3$] (3a)

2a (0.490 g, 1.08 mmol) is dissolved in THF (30 ml), and PMe_3 (150 ml, 1.45 mmol) is added. The mixture is placed in a water bath at 70°C and irradiated from a distance of 10–20 cm with a regular 300 W projector lamp until the reaction is complete (10–15 h). During this time the color of the solution changes from yellow to orange. The solvent is removed in vacuo, redissolved in ether (30 ml) and filtered over celite. The product is obtained as light yellow crystals after recrystallization from ether/hexane (0.46 g, 81.5%). IR (CH_2Cl_2, cm^{-1}): ν(CO) = 1891 (s). ^{1}H NMR: δ 1.73 (q, 3H, CCH_3), 1.51 (d, $^2J_{PH}$ = 6.6 Hz, 9H, PMe_3), 1.62 (virtual t, 3.3 Hz, 18H, PMe_3). ^{13}C NMR: δ 20.3 (d, J_{PC} = 22 Hz, PMe_3), 20.8 (virtual t, 12.5 Hz, PMe_3), 36.0 (CCH_3), 226.5 (dt, J_{PC} = 44.6 Hz, CO), 286.8 (J_{PC} = 8.5 Hz, W≡*C*). ^{31}P NMR: δ −21.4 (d, J_{PP} = 21.5 Hz, J_{WP} = 274 Hz, mutually *trans* PMe_3), −25.8 (t, J_{PP} = 21.5 Hz, J_{WP} = 220, PMe_3 *trans* to CO). *Anal.* Calc. for $WC_{12}H_{30}ClOP_3$ (0.1 ether): C, 29.20; H, 6.13. Found: C, 29.30; H, 6.04%.

5.1.9. [W(CEt)Cl(CO)(PMe$_3$)$_3$] (3b)

2b (1.930 g, 4.24 mmol) is dissolved in THF (100 ml), and PMe_3 (0.60 ml, 5.80 mmol) is added. The mixture is placed in a water bath at 70°C and irradiated from a distance of 10–20 cm with a regular 300 W projector lamp until the reaction is complete (5 h). The solvent is removed in vacuo, and the product is washed with cold (0°C) hexane. The product is purified by column chromatography at −30°C (SiO_2, eluted first with CH_2Cl_2/hexane, 1:1, then with CH_2Cl_2/THF, 98:2). The product is obtained as light yellow crystals after recrystallization from ether/hexane (1.83 g, 86.0%). IR (CH_2Cl_2, cm^{-1}): ν(CO) = 1892. ^{1}H NMR: δ 0.91 (t, 3H, CH_2CH_3), 1.51 (d, $^2J_{PH}$ = 6.6 Hz, 9H, PMe_3), 1.63 (virtual t, 3.3 Hz, 18H, 2 PMe_3), 2.0 (m, 2H, CH_2CH_3). ^{13}C NMR: δ 12.3 (CH_2CH_3), 20.4 (d, J_{PC} = 22.6 Hz, PMe_3), 20.9 (virtual t, 12.8 Hz, 2 PMe_3), 42.5 (J_{WC} = 41.5 Hz, CH_2CH_3), 226.4 (dt, $J_{PC\text{-}trans}$ = 43 Hz, $J_{PC\text{-}cis}$ = 6.5 Hz, CO), 276.5 (m, W≡*C*).

5.1.10. [W(CC$_6$H$_4$Me-4)Cl(CO)(PMe$_3$)$_3$] (3d)

2d (5–10 g) is transferred into a 250 ml Schlenk flask which is equipped with a mercury bubbler, and 100 ml PMe_3 is added. The mixture is stirred for one week, then the PMe_3 is removed under vacuum to give a yellow powder of essentially pure **3d**. Recrystallization from CH_2Cl_2/pentane gives orange crystals. IR (CH_2Cl_2, cm^{-1}): ν(CO) = 1893 (s). ^{1}H NMR: δ 1.6 (t and d, 27H, PMe_3), 2.2 (s, 3H, CH_3), 6.9 (4H, C_6H_4). ^{13}C NMR: δ 20.8, 20.9, 127.3, 128.3, 134.7, 148.7, 227.8 (dt, $^2J_{PC\text{-}trans}$ = 42.8 Hz, $^2J_{PC\text{-}cis}$ = 7.2 Hz, CO), 261.9 (t, $^2J_{PC}$ = 10.8 Hz, W≡*C*). ^{31}P NMR: δ −23.03 (d, J_{PP} = 22.0 Hz, J_{WP} = 268.2 Hz, 2 PMe_3), −26.52 (t, J_{PP} = 22.0 Hz, J_{WP} = 219.8 Hz, PMe_3). *Anal.* Calc. for $C_{18}H_{34}ClOP_3W$: C, 37.36; H, 5.92. Found: C, 37.36; H, 5.93%.

5.1.11. [W(CPh)Cl(CO)(py)(PMe$_3$)$_2$] (4c)

1c (16.675 g, 31.9 mol) is dissolved in THF (300 ml). PMe_3 (6.60 ml, 63.8 mmol) and pyridine (15 ml, 190 mmol) are added. The mixture is placed in a water bath at 70°C and irradiated from a distance of 10–20 cm with a regular 300 W projector lamp until the reaction is complete (5 h). During this time the color of the solution changes from yellow to red. The solvent is removed in vacuo, and the mixture is washed with hexane (2×25 ml). The product is obtained as dark red crystals after recrystallization from CH_2Cl_2/hexane (15.50 g, 89%).

5.1.12. [W(CC$_6$H$_4$NMe$_2$-4)Cl(CO)(py)(PMe$_3$)$_2$] (4e)

1e (5.548 g, 9.82 mol) is dissolved in THF (150 ml). PMe_3 (1.95 ml, 1.88 mmol) and pyridine (10 ml) are added. The mixture is placed in a water bath at 70°C and irradiated from a distance of 10–20 cm with a regular 300 W projector lamp until the reaction is complete (8 h). During this time the color of the solution changes from light orange to red. The mixture is filtered over celite, the solvent removed in vacuo, and the product washed with hexane (2×20 ml). The product is obtained as red crystals after recrystallization from THF/hexane (4.64 g, 77.6%). IR (CH_2Cl_2, cm^{-1}): ν(CO) = 1873. ^{1}H NMR: δ 1.38 (t, $^2J_{PH}$ = 3.3 Hz, 18H, PMe_3), 2.93 (s, 6H, Me_2N), 6.5–7.2 (m, 4H, C_6H_4), 7.8 (m, 2H, β-py), 8.1 (m, 1H, γ-py), 9.5 (m, 2H, α-py). ^{13}C NMR: δ 17.6 (PMe_3), 40.0 (Me_2N), 111.0, 123.9, 129.4, 136.5, 140.7, 147.6, 152.3 (C_6H_4, py), 238.6 (CO), 257.7 (t, J_{PC} = 11 Hz, W≡*C*). ^{31}P NMR: δ −16.7 (PMe_3).

5.1.13. [W(CMe)Cl(Me$_3$CNC)(CO)(PMe$_3$)$_2$] (5a)

3a (1.173 g, 2.33 mmol) is dissolved in methylene chloride (50 ml), and tert-butyl isocyanide (0.370 ml, 3.27 mmol) is added. The mixture is refluxed until the reaction is complete (2.5 h). No color change is observed. The solvent is removed in vacuo. The product is obtained as light orange microcrystals after recrystallization from ether/hexane (1.053 g, 89%). IR (CH_2Cl_2, cm^{-1}): ν(CN) = 2134 (m), ν(CO) = 1895 (s). ^{1}H NMR: δ 1.52 (s, 9H, CMe_3), 1.62 (virtual t, 3.2 Hz, 18H, PMe_3), 1.75 (t, $^2J_{PH}$ = 3.0 Hz, 3H, CCH_3). ^{13}C

NMR: δ 19.8 (virtual t, 13 Hz, PMe_3), 30.3 [$C(CH_3)_3$], 36.4 (CCH_3), 56.1 [$C(CH_3)_3$], 160.2 (*C*NR), 224.4 (CO), 269.9 (t, J_{PC} = 4 Hz, W≡*C*). ^{31}P NMR: δ −21.5 (J_{WP} = 281 Hz, PMe_3).

5.1.14. [W(CPh)Cl(Me$_3$CNC)(CO)(PMe$_3$)$_2$] (5b)

4c (5.312 g, 9.40 mmol) is dissolved in methylene chloride (40 ml), and tert-butyl isocyanide (1.070 ml, 9.46 mmol) is added. The solution is stirred at room temperature until the reaction is complete (1 h). During this time the color of the solution changes from red–orange to orange–brown. The solvent is removed in vacuo, and the product is washed with cold (0°C) hexane (2 × 10 ml). The product is obtained as light yellow crystals after recrystallization from THF/hexane (4.95 g, 92.5%). Crystals of X-ray quality are obtained by slow cooling of a hot saturated solution of **5b** in hexane. IR (CH_2Cl_2, cm^{-1}): ν(CN) = 2135 (m), ν(CO) = 1906 (s). ^{1}H NMR: δ 1.57 (s, 9H, CMe_3), 1.65 (virtual t, 18H, 3.6 Hz, PMe_3), 6.9–7.3 (m, 5H, Ph). ^{13}C NMR: δ 20.1 (virtual t, 13 Hz, PMe_3), 30.7 [$C(CH_3)_3$], 56.6 [$C(CH_3)_3$], 124.6, 127.5, 127.7, 151.5 (Ph), 159.1 (br, CNR), 224.9 (t, J_{PC} = 5 Hz, CO), 263.2 (t, J_{PC} = 7.5 Hz, W≡*C*). ^{31}P NMR: δ −20.8 (J_{WP} = 270 Hz). *Anal.* Calc. for $WC_{19}H_{32}ONClP_2$: C, 39.92; H, 5.64. Found: C, 40.20; H, 5.68%.

5.1.15. [W(CPh)Cl(C$_6$H$_{11}$NC)(CO)(PMe$_3$)$_2$] (5c)

4c (3.311 g, 5.83 mmol) is treated with cyclohexyl isocyanide (0.73 ml, 5.83 mmol) for 10 min as described for **5b**. The light yellow crystals from THF/hexane (3.29 g, 86.5%). IR (CH_2Cl_2, cm^{-1}): ν(CN) = 2138 (m), ν(CO) = 1907 (s). ^{1}H NMR: δ 1.4–2.1 (m, 10H, C_5H_{10}), 1.64 (virtual t, 4.5 Hz, 18H, PMe_3), 4.1 (br, 1H, CNCH), 6.95–7.1 (m, 5H, Ph). ^{13}C NMR: δ 20.1 (m, PMe_3), 22.8, 25.5, 32.6, 53.7 (C_6H_{11}), 124.5, 127.3, 127.5, 151.3 (Ph), 160.3 (br, CNR), 224.7 (CO), 263.1 (t, J_{PC} = 10.8 Hz, W≡*C*). ^{31}P NMR: δ −22.6 (J_{WP} = 276 Hz, PMe_3).

5.1.16. [W(CPh)Cl(2,6-Me$_2$C$_6$H$_3$NC)(CO)(PMe$_3$)$_2$] (5d)

4c (4.447 g, 7.84 mmol) is treated with 2,6-xylyl isocyanide (1.237 g, 9.43 mmol) for 5 min as described for **5b**. Column chromatography at −30°C (SiO_2/CH_2Cl_2). The product is redissolved in ether (20 ml) and filtered over celite. Brown solid from ether/hexane (2.05 g, 42.2%). IR (CH_2Cl_2, cm^{-1}): ν(CN) = 2095 (m), ν(CO) = 1919 (s). ^{1}H NMR: δ 1.68 (virtual t, 3.8 Hz, 18H, PMe_3), 2.50 (s, 6H, $Me_2C_6H_3$), 7.3–7.7 (m, 8H, Ph, C_6H_3). ^{13}C NMR: δ 18.5 ($Me_2C_6H_3$), 19.8 (virtual t, 13.5 Hz, PMe_3), 124.9, 127.4, 127.7, 128.0, 128.2, 128.3, 133.6, 151.1 (Ph, C_6H_3), 176.9 (CNR), 221.6 (t, J_{PC} = 5 Hz, J_{WC} = 68 Hz, CO), 264.8 (t, J_{PC} = 10.2 Hz, J_{WC} = 96 Hz, W≡*C*). ^{31}P NMR: δ −21.2 (J_{WP} = 274 Hz, PMe_3).

5.1.17. [W(CC$_6$H$_4$NMe$_2$-4)Cl(Me$_3$CNC)(CO)(PMe$_3$)$_2$] (5e)

4e (0.620 g, 1.06 mmol) is dissolved in methylene chloride (20 ml), and tert-butyl isocyanide (0.130 ml, 1.15 mmol) is added. The mixture is stirred at room temperature until the reaction is complete (30 min). During this time the color of the solution changes from red–orange to orange. The solvent is removed in vacuo, and the product is washed with hexane (2 × 10 ml). The product is obtained as an orange powder (0.430 g, 66.3%) after purification by column chromatography at −30°C (SiO_2/CH_2Cl_2). IR (CH_2Cl_2, cm^{-1}): ν(CN) = 2128 (m), ν(CO) = 1897 (s). ^{1}H NMR: δ 1.47 (s, 9H, CMe_3), 1.60 (virtual t, 3.6 Hz, 18H, PMe_3), 2.85 (s, 6H, Me_2N), 6.4–7.0 (m, 4H, C_6H_4). ^{13}C NMR: δ 20.1 (virtual t, 13.2 Hz, PMe_3), 30.6 [$C(CH_3)_3$], 40.0 (Me_2N), 56.3 [$C(CH_3)_3$], 111.1, 129.2, 141.5, 147.9 (C_6H_4), 160.7 (*C*NR), 224.8 (CO), 265.2 (t, J_{PC} = 11 Hz, W≡*C*). ^{31}P NMR: δ −22.5 (J_{WP} = 278 Hz, PMe_3).

5.1.18. [W(CPh)I(Me$_3$CNC)(CO)(PMe$_3$)$_2$] (6)

5b (2.450 g, 4.29 mmol) is dissolved in THF (40 ml), and sodium iodide (1.130 g, 7.54 mmol) is added. The solution is stirred at room temperature until the reaction is complete (45 min). During this time the color of the solution changes from light orange to orange. The solvent is removed in vacuo. The product is redissolved in methylene chloride (30 ml), and the mixture filtered over celite. The product is obtained as orange crystals after recrystallization from CH_2Cl_2/hexane (2.28 g, 88.0%). IR (CH_2Cl_2, cm^{-1}): ν(CN) = 2132 (m), ν(CO) = 1914 (s). ^{1}H NMR: δ 1.57 (s, 9H, CMe_3), 1.73 (virtual t, 3.6 Hz, 18H, PMe_3), 7.1–7.3 (m, 5H, Ph). ^{13}C NMR: δ 21.8 (m, PMe_3), 30.4 [$C(CH_3)_3$], 56.5 [$C(CH_3)_3$], 124.8, 127.0, 127.5, 150.2 (Ph), 154.8 (CNR), 222.1 (t, J_{PC} = 6.7 Hz, CO), 261.3 (t, J_{PC} = 11.0 Hz, W≡*C*). ^{31}P NMR: δ −36.6 (J_{WP} = 275 Hz, PMe_3). *Anal.* Calc. for $WC_{10}H_{32}INOP_2$: C, 34.41; H, 4.86. Found: C, 34.50; H, 4.53%.

5.1.19. [W(CHMe)Cl$_2$(CO)(PMe$_3$)$_2$] (7a)

3a (1.163 g, 2.32 mmol) is dissolved in methylene chloride (30 ml), and a light stream of HCl gas is blown over the solution until the reaction is complete (according to IR). The color of the solution changes from light yellow to brown. The solvent is removed in vacuo. The product is redissolved in ether (30 ml) and filtered over celite. The product is obtained as orange–brown crystals after recrystallization from ether/hexane (0.969 g, 90%). IR (KBr, cm^{-1}): ν(CO) = 1923. ^{1}H NMR: δ −2.36 [m, 1H, C*H*Me], 1.63 (virtual t, 3.9 Hz, 18H, PMe_3), 1.96 [m, 3H, CH*Me*]. ^{13}C NMR: δ 16.2 (virtual t, 14.7 Hz, PMe_3), 29.7 [CH(CH_3)], 224.0 [J_{PC} = 11.2 Hz, J_{CH} = 83 Hz, *C*(H)(CH_3)], 231.4 (t, CO). ^{31}P NMR: δ −19.2 (J_{WP} = 269 Hz, PMe_3). *Anal.* Calc. for $WC_9H_{22}Cl_2OP_2$ (0.2 ether): C, 24.64; H, 5.06. Found: C, 24.55; H, 4.75%.

5.1.20. [W(CHEt)Cl$_2$(CO)(PMe$_3$)$_2$] (7b)

3b (2.457 g, 4.78 mmol) is treated with HCl as described for **7a**. Column chromatography at −40°C (SiO_2, CH_2Cl_2/hexane, 3:1). Dark orange crystals from THF/hexane (1.830 g, 81%). IR (CH_2Cl_2, cm^{-1}): ν(CO) = 1937. ^{1}H NMR: δ −2.49 [t, $^2J_{PH}$ = 3.0 Hz, 1H, C*H*Et], 1.04 (t, 3H,

CH_2CH_3), 1.62 (virtual t, 4.0 Hz, PMe_3), 2.45 (m, 2H, CH_2CH_3). ^{13}C NMR: δ 13.1 (CH_2CH_3), 16.1 (virtual t, 14.5 Hz, PMe_3), 37.1 (J_{WC} = 27.6, CH_2CH_3), 231.8 (t, J_{PC} = 5.7 Hz, CO), 232.1 [t, J_{PC} = 10.8 Hz, J_{CH} = 87 Hz, CHEt]. ^{31}P NMR: δ −17.2 (J_{WP} = 270 Hz, PMe_3).

5.1.21. [W(CHPh)Cl$_2$(CO)(PMe$_3$)$_2$] (7c)

3c (2.65 g, 4.7 mmol) is dissolved in 40 ml methylene chloride, and the solution is cooled to −78°C. A light stream of HCl gas is blown over the reaction solution. Vacuum is applied, and the cooling bath is removed. (The reaction can also be conducted at room temperature, with only slightly diminished yield. Instead of gaseous HCl, a few drops of conc. HCl can be used as well. In the latter case, the reaction solution is dried with Na_2SO_4 after a few minutes reaction time, and filtered. Instead of **3c**, compound **4c** may be used as the starting material). After removal of all volatile components, the residue is redissolved in THF. The solution is filtered, and the solvent is removed under vacuum to give a microcrystalline brown solid (2.4 g, 99%). X-ray quality crystals were obtained by recrystallization from methylene chloride/pentane. M.p. 126°C (dec.); IR (CH_2Cl_2, cm^{-1}): ν(CO) = 1939 (s), (KBr, cm^{-1}): ν(CO) = 1937 (s); ^1H NMR: ($CDCl_3$, 298 K) δ 7.32 (m, 5 H, Ph), 1.67 (virtual t, 18 H, 4.0 Hz, PMe_3), −1.21 (t, 1 H, $^3J_{PH}$ = 2.8 Hz, $^2J_{WH}$ = 21.5 Hz, CHPh); ^{13}C NMR: ($CDCl_3$, 298 K) δ 233.5 (J_{WC} = 143.6 Hz, CO), 221.4 (d, J_{CH} = 82.3 Hz, J_{WC} = 78.9 Hz, CHPh), 144.1 (i-Ph), 128.7 (d, J_{CH} = 161.8 Hz, *p*-Ph), 128.5 (d, J_{CH} = 161.8 Hz, *o*-Ph), 128.0 (d, J_{CH} = 161.0 Hz, *m*-Ph), 16.1 (m, PMe_3). *Anal.* Calc. for $C_{14}H_{24}Cl_2OP_2W$: C, 32.03; H, 4.61; Cl, 13.50. Found: C, 32.15; H, 4.81; Cl, 13.20%.

5.1.22. [W(CHC$_6$H$_4$Me-4)Cl$_2$(CO)(PMe$_3$)$_2$] (7d)

3d (0.133 g, 0.23 mmol) is dissolved in 20 ml methylene chloride, and a few drops of conc. HCl are added. The reaction mixture is stirred for 15 min, then dried with Na_2SO_4, and filtered. After removal of all volatile components, the residue is redissolved in THF. The solution is filtered, and the solvent is removed under vacuum to give a microcrystalline brown solid (0.123 g, 99%). IR (CH_2Cl_2, cm^{-1}): ν(CO) = 1938 (s); ^1H NMR: ($CDCl_3$, 298 K) δ 7.15 (m, 4 H, C_6H_4), 2.37 (s, 3H, CH_3), 1.65 (virtual t, 18 H, PMe_3), −1.32 (t, 1 H, $^3J_{PH}$ = 2.7 Hz, CHTol); *Anal.* Calc. for $C_{15}H_{26}Cl_2OP_2W$: C, 33.42; H, 4.86. Found: C, 33.17; H, 5.06%.

5.1.23. [W(CHMe)Cl(Me$_3$CNC)(CO)(PMe$_3$)$_2$] CF$_3$SO$_3$ (8a)

5a (0.260 g, 0.51 mmol) is dissolved in ether (10 ml). The solution is cooled to −63°C, and triflic acid (54 ml, 0.61 mmol) is added. The bath is removed and a yellow solid forms upon warming of the solution. The mixture is centrifuged, and the supernatant decanted off. The product is washed with ether (2×5 ml). The product is obtained in nearly quantitative yield and without significant impurities (^1H NMR). IR (CH_2Cl_2, cm^{-1}): ν(CN) = 2185 (m), ν(CO) = 1992 (s). ^1H NMR: (CD_2Cl_2) δ −2.53 [m, 1H, C(H)Me], 1.15 (s, 9H, CMe_3), 1.26 (virtual t, 3 Hz, 18H, PMe_3), 1.41 (m, 3H, Me). ^{13}C NMR: (CD_2Cl_2) δ 20.8 (t, J_{PC} = 15 Hz, PMe_3), 32.7 [$C(CH_3)_3$], 35.6 [C(H)*Me*], 62.6 [$C(CH_3)_3$], 149.8 (CNR), 215.7 (CO), 241.7 [J_{CH} = 73 Hz, C(H)Me].

5.1.24. [W(CHPh)Cl(Me$_3$CNC)(CO)(PMe$_3$)$_2$] CF$_3$SO$_3$ (8b)

8b is prepared from **5b** (0.107 g, 0.19 mmol) and triflic acid (20 ml, 0.226 mmol) following the procedure described for **8a**. IR (CH_2Cl_2, cm^{-1}): ν(CN) = 2189 (m), ν(CO) = 1993 (s). ^1H NMR: (CD_2Cl_2, −30°C) δ −3.02 [t, 1H, CHPh], 1.63 (s, 9H, CMe_3), 1.77 (virtual t, 18H, PMe_3), 7.33–7.45 (m, 5H, Ph). ^{13}C NMR: (CD_2Cl_2, −30°C) δ 17.5 (PMe_3), 29.5 [$C(CH_3)_3$], 59.8 [$C(CH_3)_3$], 120.2 (q, CF_3SO_3), 128.6, 129.9, 130.3, 144.0 (Ph), 146.3 (CNR), 218.2 (CO), 230.8 (J_{CH} = 67 Hz, CHPh).

5.1.25. [W(CHPh)Cl(Me$_3$CNC)(CO)(PMe$_3$)$_2$] BF$_4$ (8c)

5b (1.090 g, 1.91 mmol) is dissolved in ether (50 ml). The solution is cooled to −78°C, and HBF_4 (85% in ether, 0.30 ml) is added. The bath is removed and a yellow solid forms upon warming of the solution. The mixture is centrifuged and the supernatant decanted off. The product is washed with ether (2×5 ml). The product is obtained in near quantitative yield (^1H NMR). Crystals of X-ray quality are obtained by slow diffusion of ether into a saturated solution of methylene chloride. IR (CH_2Cl_2, cm^{-1}): ν(CN) = 2189 (m), ν(CO) = 1993 (s). ^1H NMR: δ −2.57 [t, $^2J_{PH}$ = 6.3 Hz, 1H, CHPh], 1.70 (s, 9H, CMe_3), 1.82 (virtual t, 4.2 Hz, 18H, PMe_3), 7.3–7.6 (m, 5H, Ph). ^{13}C NMR: δ 18.2 (virtual t, 15.7 Hz, PMe_3), 30.1 [$C(CH_3)_3$], 60.5 [$C(CH_3)_3$], 129.1, 130.5, 130.9, 142.2 (Ph), 144.9 (CNR), 213.8 (CO), 230.4 (J_{CH} = 72 Hz, CHPh). ^{19}F NMR: δ −27.45 (CF_3).

5.1.26. [W(CHPh)Cl(C$_6$H$_{11}$NC)(CO)(PMe$_3$)$_2$] BF$_4$ (8d)

The procedure for the preparation of **8c** was followed. IR (CH_2Cl_2, cm^{-1}): ν(CN) = 2200 (m), ν(CO) = 1987 (s). ^1H NMR: δ −3.36 (t, $^2J_{PH}$ = 6.3 Hz, 1H, CHPh), 1.4–2.2 (m, 10H, C_5H_{10}), 1.79 (virtual t, 4.2 Hz, 18H, PMe_3), 4.0 (br, 1H, CNCH), 7.25–7.4 (m, 5H, Ph). ^{13}C NMR: (CD_2Cl_2) δ 20.7 (t, J_{PC} = 16 Hz, PMe_3), 26.2, 27.6, 35.0, 58.9 (Cy), 131.7, 132.8, 133.5, 147.2 (o, m, p, ipso, Ph), 150.2 (CNR), 215.8 (t, J_{PC} = 5.6 Hz, CO), 233.1 [t, J_{PC} = 11 Hz, J_{CH} = 75 Hz, CHPh].

5.1.27. [W(CHPh)Cl(2,6-Me$_2$C$_6$H$_3$NC)(CO)(PMe$_3$)$_2$] CF$_3$SO$_3$ (8e)

The procedure for the preparation of **8c** was followed. IR (CH_2Cl_2, cm^{-1}): ν(CN) = 2153 (m), ν(CO) = 2009 (s). ^1H NMR: (CD_2Cl_2) δ −3.04 [t, $^2J_{PH}$ = 6.9 Hz, 1H, CHPh], 1.90 (t, 18H, PMe_3), 2.55 (s, 6H, $Me_2C_6H_3$), 7.2–7.7 (m, 8H, Ph, C_6H_3). ^{13}C NMR: (CD_2Cl_2) δ 17.4 (virtual t, 15.6 Hz, PMe_3), 18.5 (Me_2Ph), 128.3, 128.7, 130.1, 130.5, 130.8, 134.9, 144.0 (Ph, C_6H_3), 162.4 (CNR), 210.9 (CO), 230.0 [J_{CH} = 72 Hz, CHPh].

5.1.28. [W(CHPh)I(Me$_3$CNC)(CO)(PMe$_3$)$_2$] CF$_3$SO$_3$ (8f)

The procedure for the preparation of **8c** was followed. IR (CH_2Cl_2, cm^{-1}): ν(CN) = 2186 (m), ν(CO) = 1987 (s).

5.1.29. [W(CHPh)I(Me$_3$CNC)(CO)(PMe$_3$)$_2$] BF$_4$ (8g)

The procedure for the preparation of **8c** was followed. IR (CH_2Cl_2, cm^{-1}): ν(CN) = 2188 (m), ν(CO) = 1987 (s). ^{1}H NMR: δ −3.01 [t, $^2J_{PH}$ = 6 Hz, 1H, C*H*Ph], 1.69 (s, 9H, CMe_3), 1.90 (virtual t, 4.2 Hz, 18H, PMe_3), 7.3–7.8 (m, 5H, Ph). ^{13}C NMR: (CD_2Cl_2) δ 22.7 (virtual t, 16.5 Hz, PMe_3), 32.4 [C(CH_3)$_3$], 63.1 [*C*(CH_3)$_3$], 131.9, 132.7, 133.8, 145.9 (Ph), 145.6 (*C*NR), 212.0 (t, J_{PC} = 6 Hz, CO), 230.2 (J_{CH} = 77 Hz, *C*HPh).

5.1.30. Deprotonation of 7c to give 9

A sample of **7c** is dissolved in CH_2Cl_2 or CD_2Cl_2 and cooled to −78°C, after which one equiv. or a small excess of pyrrolidinocyclopentene is added. The formation of [(CH$_2$)$_4$C=N(CH$_2$)$_4$][W(CPh)Cl$_2$(CO)(PMe$_3$)$_2$] (**9**) is confirmed by IR and NMR spectroscopy. Complex **9** is not stable at room temperature. IR (CH_2Cl_2, cm^{-1}): ν(CO) = 1833 (s). ^{1}H NMR: δ 1.9 (m, 4H), 2.8 (m, 4H), 2.9 (m, 4H), 3.8 (m, 4H) ([(CH$_2$)$_4$C=N(CH$_2$)$_4$)]$^+$). ^{13}C NMR: (CD_2Cl_2, −60°C) δ 24, 36, 43, 55, 195 ([(CH$_2$)$_4$C=N(CH$_2$)$_4$)]$^+$), 245.1 (s, J_{WC} = 180 Hz, CO), 256.3 (t, $^2J_{PC}$ = 11.7 Hz, J_{WC} = 194 Hz, *C*Ph). ^{31}P NMR: (CD_2Cl_2, −60°C) δ −12.63 (J_{WP} = 288 Hz, PMe_3).

5.1.31. Deprotonation of 7c and subsequent addition of pyridine, CNCMe$_3$ and P(OMe)$_3$ to afford 4c, 5b and 10

A solution of a small amount of **7c** in THF is cooled to −78°C, and 1.1 equiv. of n-BuLi in hexane is added. After stirring for 30 min at this temperature, a two-fold excess of pyridine or $CNCMe_3$ is added, and the solution is allowed to warm to room temperature. After stirring for 30 min at room temperature, the solvent is removed under vacuum. The spectroscopic parameters of the products are in agreement with those of authentic samples of **4c** and **5b**. **10**: A solution of **7c** (0.148 g, 0.28 mmol) in THF is cooled to −78°C, and 1.2 equiv. of n-BuLi in hexane (1.6 M, 0.21 ml, 0.34 mmol) is added. After stirring for 30 min at this temperature, trimethylphosphite (0.84 g, 0.08 ml, 2.4 equiv.) is added, and the solution is allowed to warm to room temperature. After stirring for 30 min at room temperature, the solvent is removed under vacuum. The residue is redissolved in CH_2Cl_2, the resulting solution is filtered, and the solvent is removed under vacuum to give an orange oil. The oily product is washed with hexane and dried under vacuum. Yield: 0.159 g, 92%. IR (CH_2Cl_2, cm^{-1}): ν(CO) = 1916 (s). ^{1}H NMR: δ 1.70 (virtual t, 18 H, PMe_3), 3.73 (9H, J_{PH} = 11.1 Hz, P(OMe)$_3$), 7.13 (m, 5H, C_6H_5).

5.2. Crystallographic studies

5.2.1. Neutron diffraction study of 7a

Crystals were obtained by slow recrystallization from ether/hexane. A yellow–brown specimen of volume 2.7 mm^3 was mounted on an aluminum pin with halocarbon grease and sealed under a helium atmosphere inside an aluminum container. This container was placed in a closed-cycle helium refrigerator (DISPLEX® Model CS-202. APD Cryogenics, Inc.) and mounted on the four-circle diffractometer at port H6S of the High Flux Beam Reactor at Brookhaven National Laboratory. The neutron beam, monochromated by Ge (220) planes in transmission geometry, was of wavelength 1.15863(8) Å as calibrated against a KBr crystal (a_o = 6.6000 Å at 295 K). The sample temperature was maintained at 15.0 ± 0.1 K during the experiment, and unit cell dimensions were determined by least-squares fit of $\sin^2\theta$ values for 32 reflections in the range $52° < 2\theta < 60°$. Intensity data were obtained over one quadrant of reciprocal space by means of ω–2θ scans. The intensities of two reflections were monitored during the data collection and showed no systematic variations throughout. Integrated intensities I_o and variances $\sigma^2(I_o)$ were derived from the scan profiles as described previously [43]. Lorentz factors were applied, as well as an analytical absorption correction [44,45]. Transmission factors were in the range 0.625–0.744. Averaging over 154 symmetry-related pairs of reflections resulted in an internal agreement factor of 0.016 and yielded 4003 independent observations, of which 476 were negative, 4 being less than $-4\sigma(F_o^2)$. Further details are given in Table 1.

Initial coordinates were obtained from the X-ray structure determination. Coherent neutron-scattering lengths (*fm*) for H (−3.7409), C (6.6484), O (5.803), P (5.13), Cl (9.579) and W (4.77) were taken from the tabulation of Koester [46]. Least-squares refinements were carried out by a full-matrix procedure [47], minimizing $\Sigma w|F_o^2 - (k^2F_c^2|^2$, where $w = [\sigma^2(F_o^2) + (0.02F_o^2)^2]^{-1}$, using all independent data except for 7 reflections, which were affected by the powder lines from the aluminum container. The final model included the scale factor k, positional and anisotropic displacement parameters β_{ij} for all atoms and the isotropic type I extinction parameter [48]. This gave a total of 335 variable parameters. The refinement converged ($\Delta p_i/\sigma(p_i) < 0.1$) with fit indices $R(F_o^2) = 0.157$, $R_w(F_o^2) = 0.141$, $R_w(F_o) = 0.099$, GOF = 1.21, based on 3996 reflections. The isotropic extinction parameter $y = 2.7(3) \times 10^3$. Eleven reflections had an extinction correction larger than 1.1, the largest being 1.22 for (302). In the final difference Fourier map, the largest $|\Delta\rho|$ errors were about 3% of the maximum peak in the ρ_o map. The structure shown in Fig. 2 was drawn using ORTEP [49].

5.2.2. X-ray diffraction studies of 5b, 7a, and 8c

Selected crystallographic data are listed in Table 1. The general procedures for unit cell determination, data collection, and structure solution have previously been described in detail [50]. The intensity measurements were made on an Enraf-Nonius CAD4A automated diffractometer, using a variable-rate, ω–2θ scan technique. Empirical absorption corrections (DIFABS) [51] were applied. All calculations were performed using the TEXSAN programs [52]. The structures were solved by direct methods and difference Fourier pro-

cedures. For **8c**, the intensities of three reflections, which were measured after every 60 min of X-ray exposure, declined by 27.40%. A linear correction factor was applied.

5.2.3. X-ray diffraction study of 7c

Selected crystallographic data are listed in Table 1. The structure was solved by standard heavy atom techniques. The methyl carbon atoms of both trimethylphosphine groups were disordered between two positions. The occupancies were allowed to vary as x and $1-x$ and refined to the values 0.53, 0.47 for one trimethylphosphine and 0.62, 0.38 for the second. The phenyl hydrogen atoms and H(8) were located on difference Fourier maps following refinement of the nonhydrogen atoms. The phenyl hydrogen positions were subsequently idealized with C–H = 0.968 and $B(H) = 1.2 \times B(C)$. In the final cycles of blocked-cascade least-squares refinement, all nonhydrogen atoms, except those on the disordered methyl groups, were assigned anisotropic temperature factors, the methyl carbon atoms were given isotropic temperature factors, H(8) was held fixed and a riding model was used for the phenyl hydrogens. The quantity minimized in the least-squares procedure was $\sum w(|F_o| - |F_c|)^2$ where w is the weight of a given observation ($w^{-1} = \sigma^2(|F_o|) + g|F_o|^2$, final value of $g = 0.00028$). The analytical forms for the scattering factors of the neutral atoms were used [53]. Final refinement with 177 parameters converged at $R = 0.035$ and $R_w = 0.035$ with goodness of fit = 1.70.

6. Supplementary material

Further details of the crystal structure investigations of complexes **5b**, **7a**, **7c**, and **8c** may be obtained from the authors upon request.

Acknowledgements

Support for this work by the National Science Foundation is gratefully acknowledged. We thank R. Subramanian for work on the crystal structure analyses of **5b** and **8c**. The neutron diffraction study of **7a** was carried out at Brookhaven National Laboratory under contract DE-AC02-98CH10886 with the US Department of Energy and supported by its Office of Basic Energy Sciences. We thank C. Koehler, III for technical assistance.

References

[1] (a) E.O. Fischer, Angew. Chem. 86 (1974) 651; E.O. Fischer, Adv. Organomet. Chem. 14 (1976) 1; (b) E.O. Fischer, U. Schubert, J. Organomet. Chem. 100 (1975) 59; (c) H. Fischer, P. Hofmann, F.R. Kreissl, R.R. Schrock, U. Schubert, K. Weiss, Carbyne Complexes, VCH, Weinheim, 1988; (d) H.P. Kim, R.J. Angelici, Adv. Organomet. Chem. 27 (1987) 51; (e) R.R. Schrock, Acc. Chem. Res. 19 (1986) 342; (f) M.A. Gallop, W.R. Roper, Adv. Organomet. Chem. 25 (1986) 121; (g) F.G.A. Stone, Adv. Organomet. Chem. 31 (1991) 53; (h) A. Mayr, H. Hoffmeister, Adv. Organomet. Chem. 32 (1991) 227; (i) A. Mayr, C.M. Bastos, Prog. Inorg. Chem. 40 (1992) 1; (j) P.F. Engel, M. Pfeffer, Chem. Rev. 95 (1995) 2281; (k) A. Mayr, S. Ahn, Adv. Trans. Met. Coord. Chem. 1 (1996) 1; (l) R.A. Henderson, Angew. Chem. 108 (1996) 1049; Angew. Chem., Int. Ed. Engl. 35 (1996) 947; (m) L. McElwee-White, Synlett. (1996) 806.

[2] (a) F.R. Kreissl, W.J. Sieber, M. Wolfgruber, J. Riede, Angew. Chem. 96 (1984) 618; Angew., Chem. Int. Ed. Engl. 23 (1984) 640; (b) F.R. Kreissl, W.J. Sieber, H. Keller, J. Riede, M. Wolfgruber, J. Organomet. Chem. 320 (1987) 83; (c) J.A.K. Howard, J.C. Jeffery, S. Li, F.G.A. Stone, J. Chem. Soc., Dalton Trans. (1992) 627; (d) J.C. Jeffery, S. Li, F.G.A. Stone, J. Chem. Soc., Dalton Trans. (1992) 635; (e) K.B. Kingsbury, J.D. Carter, A. Wilde, H. Park, F. Takusagawa, L. McElwee-White, J. Am. Chem. Soc. 115 (1993) 10 056; (f) M.D. Mortimer, J.D. Carter, L. McElwee-White, Organometallics 1 (1993) 4493.

[3] J.A.K. Howard, J.C. Jeffery, J.C.V. Laurie, I. Moore, F.G.A. Stone, A. Stringer, Inorg. Chim. Acta 100 (1985) 23.

[4] K.E. Garrett, J.B. Sheridan, D.B. Pourreau, W.C. Feng, G.L. Geoffroy, D.L. Staley, A.L. Rheingold, J. Am. Chem. Soc. 111 (1989) 8383.

[5] (a) A.C. Filippou, W. Grünleitner, Z. Naturforsch., Teil B 44 (1989) 1023; (b) E.M. Carnahan, S.J. Lippard, J. Am. Chem. Soc. 114 (1992) 4166; (c) J.J.R. Fraústo Da Silva, M.A. Pellinghelli, J.A.L. Pombeiro, R.L. Richards, A. Tiripicchio, Y. Wang, J. Organomet. Chem. 454 (1993) C8.

[6] (a) S.A. Brew, F.G.A. Stone, Adv. Organomet. Chem. 35 (1993) 135; (b) A.P. James, F.G.A. Stone, J. Organomet. Chem. 310 (1986) 47.

[7] (a) F.R. Kreissl, W.J. Sieber, M. Wolfgruber, J. Organomet. Chem. 270 (1984) C45; (b) H.P. Kim, S. Kim, R.A. Jacobson, R.J. Angelici, Organometallics 3 (1984) 1124; (c) R.A. Doyle, R.J. Angelici, Organometallics 8 (1989) 2207; (d) M. Etienne, P.S. White, J.L. Templeton, J. Am. Chem. Soc. 113 (1991) 2324; (e) J.C. Jeffery, F.G.A. Stone, G.K. Williams, Polyhedron 10 (1991) 215; (f) G.C. Bruce, F.G.A. Stone, Polyhedron 11 (1992) 1607.

[8] (a) P.R. Sharp, S.J. Holmes, R.R. Schrock, M.R. Churchill, H.J. Wasserman, J. Am. Chem. Soc. 103 (1981) 965; (b) S.J. Holmes, R.R. Schrock, J. Am. Chem. Soc. 103 (1981) 4599; (c) S.J. Holmes, D.N. Clark, H.W. Turner, R.R. Schrock, J. Am. Chem. Soc. 104 (1982) 6322; (d) M.R. Churchill, H.J. Wasserman, H.W. Turner, R.R. Schrock, J. Am. Chem. Soc. 104 (1982) 1710; (e) M. Green, A.G. Orpen, I.D. Williams, J. Chem. Soc., Chem. Commun. (1982) 493; (f) M. Bottrill, M. Green, A.G. Orpen, D.R. Saunders, I.D. Williams, J. Chem. Soc., Dalton Trans. (1989) 511.

[9] A. Mayr, M.F. Asaro, M.A. Kjelsberg, K.S. Lee, D. Van Engen, Organometallics 6 (1987) 432.

[10] C.M. Bastos, N. Daubenspeck, A. Mayr, Angew. Chem. 105 (1993) 793; Angew. Chem., Int. Ed. Engl. 32 (1993) 743.

[11] (a) E.O. Fischer, A. Maasböl, Chem. Ber. 100 (1967) 2445; (b) E.O. Fischer, A. Ruhs, F.R. Kreissl, Chem. Ber. 110 (1977) 805.

[12] (a) A. Mayr, G.A. McDermott, A.M. Dorries, Organometallics 4 (1985) 608; (b) G.A. McDermott, A.M. Dorries, A. Mayr, Organometallics 6 (1987) 925.

[13] (a) A. Mayr, T.-Y. Lee, M.A. Kjelsberg, K.S. Lee, Organometallics 13 (1994) 2512; (b) P. Steil, A. Mayr, Z. Naturforsch., Teil B 47 (1992) 656.

[14] (a) L.M. Atagi, S.C. Critchlow, J.M. Mayer, J. Am. Chem. Soc. 114 (1992) 9223.

[15] E.O. Fischer, T.L. Lindner, F.R. Kreissl, P. Braunstein, Chem. Ber. 110 (1977) 3139.

[16] J.H. Wengrovius, R.R. Schrock, M.R. Churchill, H.J. Wasserman, J. Am. Chem. Soc. 104 (1982) 1739.

[17] A.J. Bondi, J. Chem. Phys. 68 (1964) 441.

[18] M.R. Churchill, H.J. Wasserman, Inorg. Chem. 22 (1983) 1574.

[19] A. Mayr, C.M. Bastos, J. Am. Chem. Soc. 112 (1990) 7797.

[20] (a) N.M. Kostić, R.F. Fenske, Organometallics 1 (1982) 489; (b) J. Ushio, H. Nakatsuji, T. Yonezawa, J. Am. Chem. Soc. 106 (1984) 5892.
[21] A. Mayr, Comm. Inorg. Chem. 10 (1990) 227.
[22] A. Mayr, K.S. Lee, M.A. Kjelsberg, D. Van Engen, J. Am. Chem. Soc. 108 (1986) 6079.
[23] A.J. Schultz, R.K. Brown, J.M. Williams, R.R. Schrock, J. Am. Chem. Soc. 103 (1981) 169.
[24] J. Espuelas, M.A. Esteruelas, F.J. Lahoz, L.A. Oro, N. Ruiz, J. Am. Chem. Soc. 115 (1993) 4683.
[25] P. Schwab, R.H. Grubbs, J.W. Ziller, J. Am. Chem. Soc. 118 (1996) 100.
[26] A. Höhn, H. Werner, J. Organomet. Chem. 255 (1990) 382.
[27] G.R. Clark, K. Marsden, W.R. Roper, L.J. Wright, J. Am. Chem. Soc. 102 (1980) 6570.
[28] M. Brookhart, M.L.H. Green, L.-L. Wong, Prog. Inorg. Chem. 36 (1988) 1.
[29] J.H. Freudenberger, R.R. Schrock, Organometallics 4 (1985) 1937.
[30] T.G. Appleton, H.C. Clark, L.E. Manzer, Coord. Chem. Rev. 10 (1973) 335.
[31] J. Feldman, R.R. Schrock, Prog. Inorg. Chem. 39 (1991) 1.
[32] (a) R. Taylor, O. Kennard, J. Am. Chem. Soc. 104 (1982) 5063; (b) L. Brammer, J.M. Charnock, P.L. Goggin, R.J. Goodfellow, A.G. Orpen, T.F. Koetzle, J. Chem. Soc., Dalton Trans. (1991) 1789.
[33] A. Albinati, V.I. Bakhmutov, K.G. Caulton, E. Clot, J. Eckert, O. Eisenstein, D.G. Gusev, V.V. Grushin, B.E. Hauger, W.T. Klooster, T.F. Koetzle, R.K. McMullan, T.J. O'Loughlin, M. Pélissier, J.S. Ricci, M.P. Sigalas, A.B. Vymenits, J. Am. Chem. Soc. 115 (1993) 7300.
[34] S.G. Feng, P.S. White, J.L. Templeton, J. Am. Chem. Soc. 112 (1990) 8192.
[35] A. Mayr, M.F. Asaro, T.J. Glines, D. Van Engen, G.M. Tripp, J. Am. Chem. Soc. 115 (1993) 8187.
[36] J.L. Templeton, Adv. Organomet. Chem. 29 (1989) 1.
[37] A. Mayr, C.M. Bastos, R.T. Chang, J.X. Haberman, K.S. Robinson, D.A. Belle-Oudry, Angew. Chem. 104 (1992) 802; Angew. Chem., Int. Ed. Engl. 31 (1992) 747.
[38] K.H. Dötz, H. Fischer, P. Hofmann, F.R. Kreissl, U. Schubert, K. Weiss, Transition Metal Carbene Complexes, Verlag Chemie, Weinheim, 1983.
[39] R.J. Goddard, R. Hoffmann, E.D. Jemmis, J. Am. Chem. Soc. 102 (1980) 7667.
[40] (a) D.C. Brower, K.R. Birdwhistell, J.L. Templeton, Organometallics 5 (1986) 94; (b) W.J. Sieber, M. Wolfgruber, N.H. Tran-Huy, H.R. Schmidt, H. Heiss, P. Hofmann, F.R. Kreissl, J. Organomet. Chem. 341 (1988) 340.
[41] P.J. Brothers, Prog. Inorg. Chem. 28 (1981) 1.
[42] G.J. Kubas, Acc. Chem. Res. 21 (1988) 120.
[43] R.K. McMullan, J. Epstein, J.R. Ruble, B.M. Craven, Acta Crystallogr., Sect. B 35 (1979) 688.
[44] J. de Meulenaer, H. Tompa, Acta Crystallogr. 19 (1965) 1014.
[45] L.K. Templeton, D.H. Templeton, Abstr. Am. Crystallogr. Assoc. Meet., Storrs, CT, 1973, p. 143.
[46] L. Koester, Springer Tracts Mod. Phys. 80 (1977) 36.
[47] J.-O. Lundgren, Crystallographic Computer Programs, Rep. UUIC-B13-4-05, Institute of Chemistry, University of Uppsala, Sweden, 1982.
[48] P.J. Becker, P. Coppens, Acta Crystallogr., Sect. A 30 (1974) 129.
[49] C.K. Johnson, ORTEP II, Report ORNL-5138, Oak Ridge National Laboratory, TN, 1976
[50] S. Lincoln, S.A. Koch, Inorg. Chem. 25 (1986) 1594.
[51] N. Walker, D. Stuart, Acta Crystallogr., Sect. A 39 (1983) 158.
[52] Single Crystal Structure Analysis Software, Version 1.6, Molecular Structure Corporation, The Woodlands, TX, 1993.
[53] International Tables of X-ray Crystallography, Vol. IV, Kynoch, Birmingham, UK, 1975, pp. 99, 149.